

**Tropical Cyclone Intensity Change -  
A Quantitative Forecasting Scheme**

by  
Kenneth M. Dropco

Department of Atmospheric Science  
Colorado State University  
Fort Collins, Colorado

P.I. William M. Gray

**Colorado  
State  
University**

**Department of  
Atmospheric Science**

Paper No. 333



TROPICAL CYCLONE INTENSITY CHANGE - A  
QUANTITATIVE FORECASTING SCHEME

By

Kenneth M. Dropco

Department of Atmospheric Science

Colorado State University

Fort Collins, Colorado

80523

May, 1981

Atmospheric Science Paper No. 333

1870

1871

1872

1873

1874

## ABSTRACT

This paper discusses one to two day future tropical cyclone intensity change from both a composite and an individual case point-of-view. Tropical cyclones occurring in the Gulf of Mexico during the period 1957-1977 form the primary data source. A dense rawinsonde data network to the poleward side of storms in this region allows more quantitative evaluation of the environment of individual storm cases than is possible in other regions.

Weather charts of the NW Atlantic were initially examined in hopes of finding common meteorological parameters which were different between the intensifying and non-intensifying cyclones. Few obvious and consistent differences could be found. A rawinsonde composite analysis was then performed to investigate mean differences between these two classes of systems. By contrast to the individual case analysis, composite differences were detected in the 200 mb height fields, the 850 mb temperature fields, the 200 mb zonal wind and the vertical shears of the zonal wind. The individual cyclones which make up the composite study were then separately examined using this composite case knowledge. Similar parameter differences were found in a majority of individual cases.

A cyclone intensity change forecast scheme was developed from the results of the individual storm systems. This forecast scheme was then tested against independent storm cases. Correct predictions of intensification or non-intensification could be made approximately 75% of the time. The scheme was also tested on other rawinsonde composite data sets in other ocean basins. Again, the results were highly significant. A favorable strength of this scheme is the quantitative cyclone intensity change index which is developed from purely objective techniques.

All results indicate a relationship between intruding baroclinic zones and subsequent storm weakening or lack of further storm intensification. The forecast scheme measures those parameters most affected by such baroclinic interaction and allows a prediction of future 18 to 42 hour intensity change.

TABLE OF CONTENTS

	Page
1. INTRODUCTION . . . . .	1
1.1 Compositing Philosophy . . . . .	3
1.2 Compositing Technique. . . . .	4
1.3 Data Set . . . . .	7
2. RAWINSONDE COMPOSITE COMPARISON: INTENSIFYING VS. NON- INTENSIFYING. . . . .	14
2.1 Climatological Differences . . . . .	14
2.2 Storm Movement . . . . .	15
2.3 Thermodynamic Parameters . . . . .	17
2.4 Dynamic Differences . . . . .	22
2.5 Summary of Composite Results . . . . .	31
3. DEVELOPMENT OF THE INTENSITY CHANGE FORECASTING SCHEME .	32
3.1 Selection of Parameters. . . . .	32
3.2 Application of Parameters to Individual Cases . .	36
3.3 Designation of the Forecasting Parameter . . . . .	40
3.4 Rate of Change of IP . . . . .	43
4. APPLICATION OF IP TO INDEPENDENT DATA . . . . .	45
4.1 Results of Independent Storm Analysis . . . . .	45
4.2 Climatological and Diurnal Variations of the Parameters. . . . .	49
4.3 Comparative Composite Analysis . . . . .	50
5. STATISTICAL ANALYSIS . . . . .	58
5.1 Contingency tables . . . . .	58
5.2 Prefigurance - Post Agreement . . . . .	60
5.3 Skill Scores . . . . .	61
5.4 MRPP . . . . .	63
6. CONCLUSION . . . . .	65
REFERENCES. . . . .	70
APPENDIX A . . . . .	74
APPENDIX B -- COMPUTATIONAL PROCEDURES FOR THE INTENSITY CHANGE FORECASTING PARAMETER . . . . .	83
APPENDIX C -- DESCRIPTION OF COMPOSITE DATA SETS . . . . .	87



## 1. INTRODUCTION

Despite all the recent advances in electronic computer and satellite technologies, tropical cyclone intensity change forecasting skill has not shown much improvement (Hebert, 1978). The computer has made more meteorological products available and the satellite has made us more aware of the location, movement and cloudiness of tropical systems. However, neither of these technological developments has led to significant improvements in the cyclone intensity change forecast skill. More research into the physics of this process is needed.

In general, tropical cyclone intensity change appears to be associated with both internal and external storm mechanisms such as that given in Eq. 1:

$$\frac{\partial I}{\partial t} = A + B + C \quad (1)$$

where  $I$  = cyclone intensity,  $A$  = inner core ( $0-3^\circ$  radius) mesoscale influences on cyclone intensity change,  $B$  = outer region ( $3-12^\circ$  radius) synoptic scale influences, and  $C$  = global scale ( $> 12^\circ$  radius) interaction and feedback influences on cyclone intensity change. We might view the typical time scales of these intensity change influences to be approximately 0-12 hours for influence  $A$ , 12-48 hours for influence  $B$  and  $> 48$  hours for influence  $C$ . Limited conventional observations of the inner core do not allow us to routinely measure the inner core physical parameters which likely lead to short time scale intensity change. However, new satellite cloudiness analysis techniques by the National Oceanic and Atmospheric Administration/National Environmental Satellite Service NOAA/NESS), National Aeronautic and Space Administration (NASA), and the Naval Environmental Prediction Research Facility (NEPRF) satellite groups are beginning to show some promising

correlations on the shorter time scale. New evidence by E. Núñez (1981) indicates that the storm outer region environment has the most significant effect on 1-2 day future intensity change. Therefore, this study examines the surrounding outer region environmental influences (effect B in Eq. 1) to determine how they act to influence future prediction of cyclone intensity change. As more becomes known about both inner and outer region storm characteristics and storm intensity, further improvement of cyclone intensity forecast skill may be possible through a combination of both inner and outer storm intensity change relationships.

The recent research findings of E. Núñez (1981) on tropical cyclone intensity change form the general background informational base for the initiation of this study. Núñez (1981) examined cyclone intensity change by comparing rawinsonde composited cases of deepening versus filling tropical cyclones in the northwest Pacific and northwest Atlantic. However, he did not deal with individual cases of cyclone change. His results were that filling systems had stronger middle and upper level height and temperature gradients on their poleward side. Often a middle and upper level trough existed to the northwest of the filling storm center that was not present with the growing or steady systems. He attributed the differences between the filling/deepening data sets to strong baroclinic interaction on the north and northwest octants of the storm.

Based on the Núñez composite data results, the authors have undertaken the investigation of such baroclinic interaction on an individual case basis. Tropical cyclones in the Gulf of Mexico were selected because of the abundance of data on the poleward side of these systems. Storms were stratified as intensifying and non-intensifying.

It was hoped that the effects of large scale baroclinic interaction on the north side of the non-intensifying cyclones systems would produce evidence of intensity change that could be recognized from the weather charts. But after hours of detailed analysis of upper and lower tropospheric weather charts, the authors became convinced that individual weather charts by themselves did not provide obvious and consistent quantitative differences which would signal intensity change. Although the presence of trough interaction was observed it was difficult to quantify the effects of that interaction solely from comparisons of individual weather charts. Therefore, rawinsonde composites were formed for both data sets. The rawinsonde composite techniques developed at Colorado State University (CSU) were then used to determine the major physical differences between systems. The knowledge gained from this comparative composite study was then tested in individual cases to determine the extent to which such differences could be detected in each particular forecast situation. Such differences were found in about three-quarters of the cases. A purely objective and quantitative scheme for forecasting tropical cyclone intensity change was then devised. Independent data were selected to further test the forecast scheme. A thorough statistical analysis was made of all the sampled data.

### 1.1 Compositing Philosophy

The Gulf of Mexico is one of the best locations in the world to study individual storms because of the abundance of surface and upper air observing sites throughout the Caribbean and southeastern United States (Fig. 1). But, even in the Gulf of Mexico problems arise because of the sparcity of data over Mexico and the lack of observations within the center of the Gulf. The routine observational data is often augmented by aircraft observations but these data are often limited to inner core information and rarely at more than one or two levels. The compositing technique allows us to overlook these short-

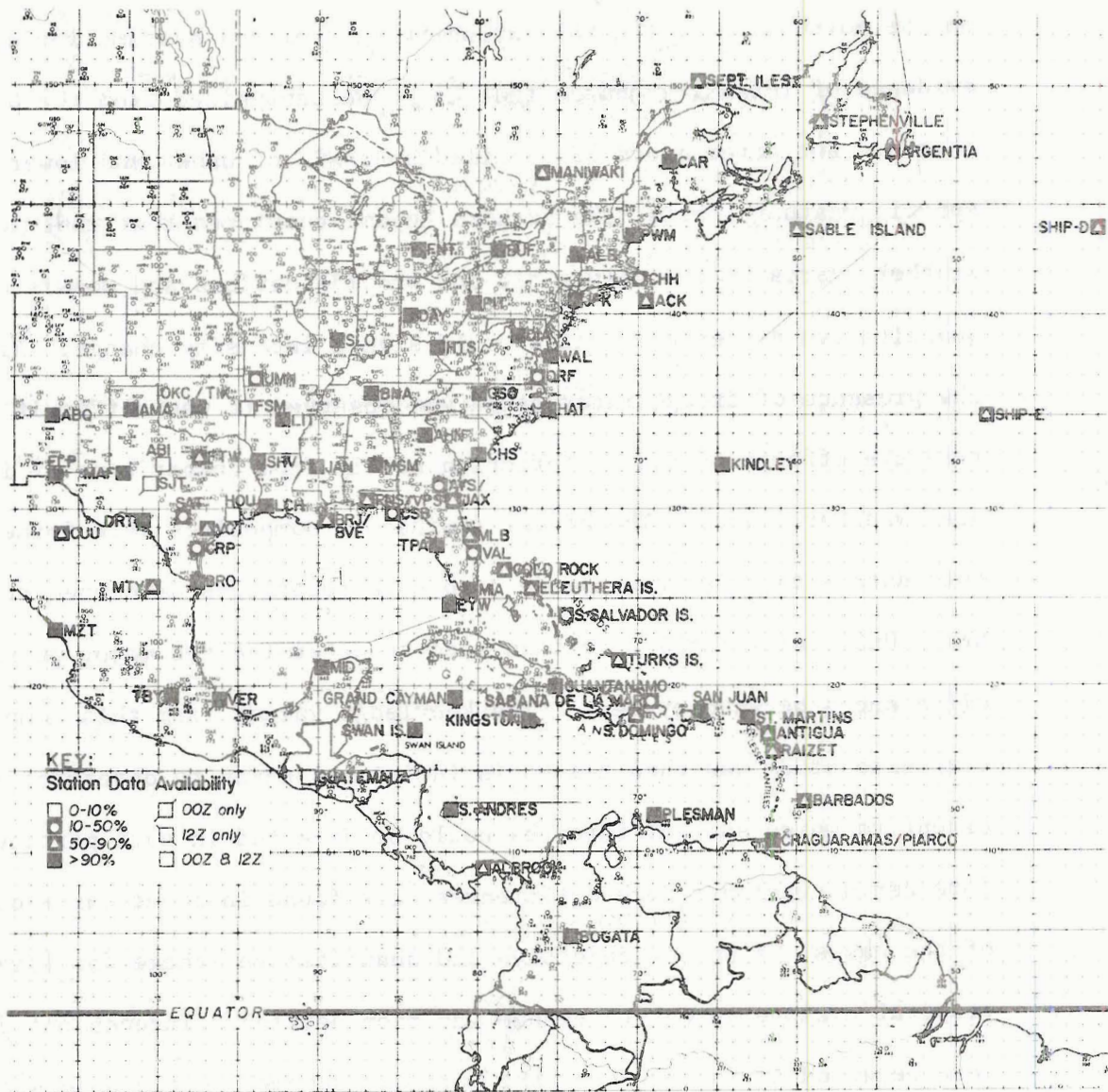


Fig. 1. West Atlantic rawinsonde data network utilized in the present study.

comings by using rawinsonde data for many cyclones which show similar characteristics.

The composite technique tends to smooth over many of the individual characteristics and diurnal variations of a single storm. Still, by proper data selection and handling techniques, we can gain valuable information on storm class differences. Once such differences are found they can then be applied to the individual cases to see how representative the composite differences are.

## 1.2 Compositing Technique

The composite is accomplished by positioning a cylindrical grid with a radius of  $15^{\circ}$  latitude at the surface center of the storm for each time period. The grid consists of 21 vertical levels extending from the surface to 50 mb. The horizontal grid is divided into eight octants and eight radial belts as depicted in Fig. 2. This subdivision yields 64 boxes whose areal extent increases radially outward.

By using this grid system over every storm in our set, we can accumulate many values of each parameter in each of the 64 boxes. The accumulated values in each grid box are averaged and the value is assigned to represent the corresponding box. Repeating this averaging process for each of the meteorological parameters in each of the 64 grid boxes yields the basic structure for the composited cyclone.

The observed or computed parameters include 14 dynamic and 10 thermodynamic parameters as listed below:

<u>Dynamic Parameters</u>	<u>Thermodynamic Parameters</u>
u (zonal wind)	T (temperature)
v (meridional wind)	$T_v$ (virtual temperature)
$V_r$ (radial wind)	$\theta$ (potential temperature)
$V_{\theta}$ (tangential wind)	Z (height)
$V_p$ (wind parallel to storm motion)	RH (relative humidity)
$V_n$ (wind normal to storm motion)	q (specific humidity)
$V_r f_r$ (Coriolis torque)	s (static energy)
$V_r q_c$ (horizontal moisture transport)	h (moist static energy)
DIV (divergence)	$h^*$ (saturated moist static energy)
$\omega$ (vertical motion)	$\frac{\partial gz}{\partial r}$ (radial height gradient)
$q_c \omega$ (vertical moisture transport)	
$\zeta$ (vorticity)	
$\frac{\partial u}{\partial p}$ (vertical zonal wind shear)	

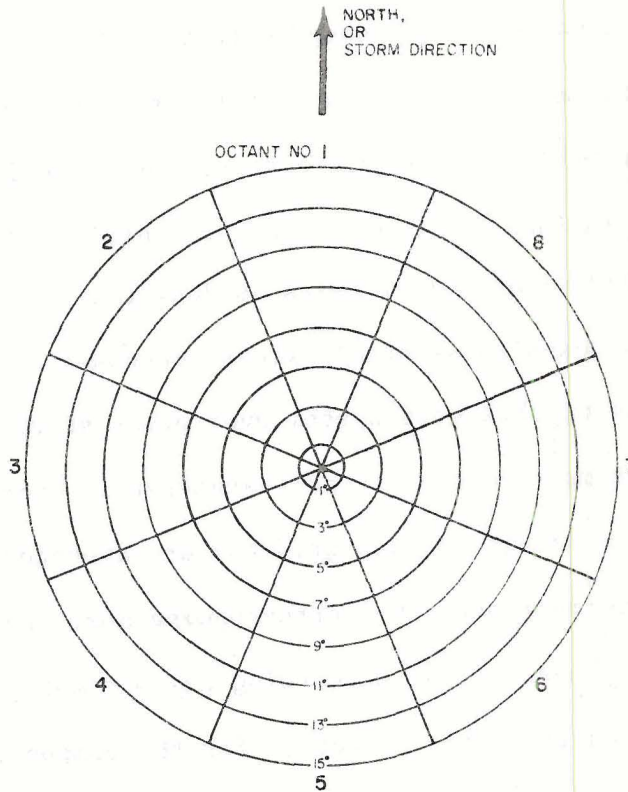


Fig. 2. Compositing grid. Arrow points north.

All parameters were examined in this study but only the zonal wind, vertical shear of the zonal wind, height and temperature were found to exhibit strong differences between the intensifying and non-intensifying cyclone systems.

Corrections in the relative position of the rawinsonde to the storm center are made by assuming the balloon is released 30 minutes prior to the scheduled observation time and that the ascent rate is  $5 \text{ m s}^{-1}$ . Drift corrections are then made by using the reported wind profiles. Computational procedures also correct for translational movement of the storm while the balloon is airborne.

The computer programs are designed to composite in four different cylindrical coordinate systems, but this study will be limited to the natural (NAT) coordinate system. In this coordinate system the compositing grid is stationary with respect to the storm center. Octant 1 is

always pointing to the north, regardless of the storm's direction of movement.

### 1.3 Data Set

This study utilizes 21 years (1957-1977) of northwest Atlantic rawinsonde data from the stations shown in Fig. 1. The data come from the Northern Hemisphere Data Tabulations (NHDT) tapes from Asheville, North Carolina Records Center which was made available to the Colorado State University (CSU) project courtesy of Mr. Roy Jenne and his group at the National Center for Atmospheric Research (NCAR) in Boulder, CO. Both 00 and 12 GMT soundings were used.

The cyclones were selected from the official best track positions of the National Hurricane Center. The cyclones were chosen if they made landfall along the Gulf Coast of the United States from approximately 100 miles south of Brownsville, TX to the Florida Keys. Cyclones were stratified into intensifying or non-intensifying data sets based on their maximum wind speed changes for the time they were in the Gulf. A cyclone was considered an intensifier if it had a wind speed increase of greater than 20 knots (kts) in a 24 hour period within 42 hours of landfall (see Figs. 3 and 4). There were seven cyclones which were classified as intensifying but showed a significant filling a few hours prior to landfall. These storms were not considered in this study. A complete listing of all cyclones which make up the two data sets is shown in Table 1. Table 1 also lists the cyclone's maximum sustained wind speed for the LF -42, LF -18 and landfall time periods (LF represents Land Fall). The average intensity of the intensifying cyclones is nearly twice as strong as the non-intensifying systems.

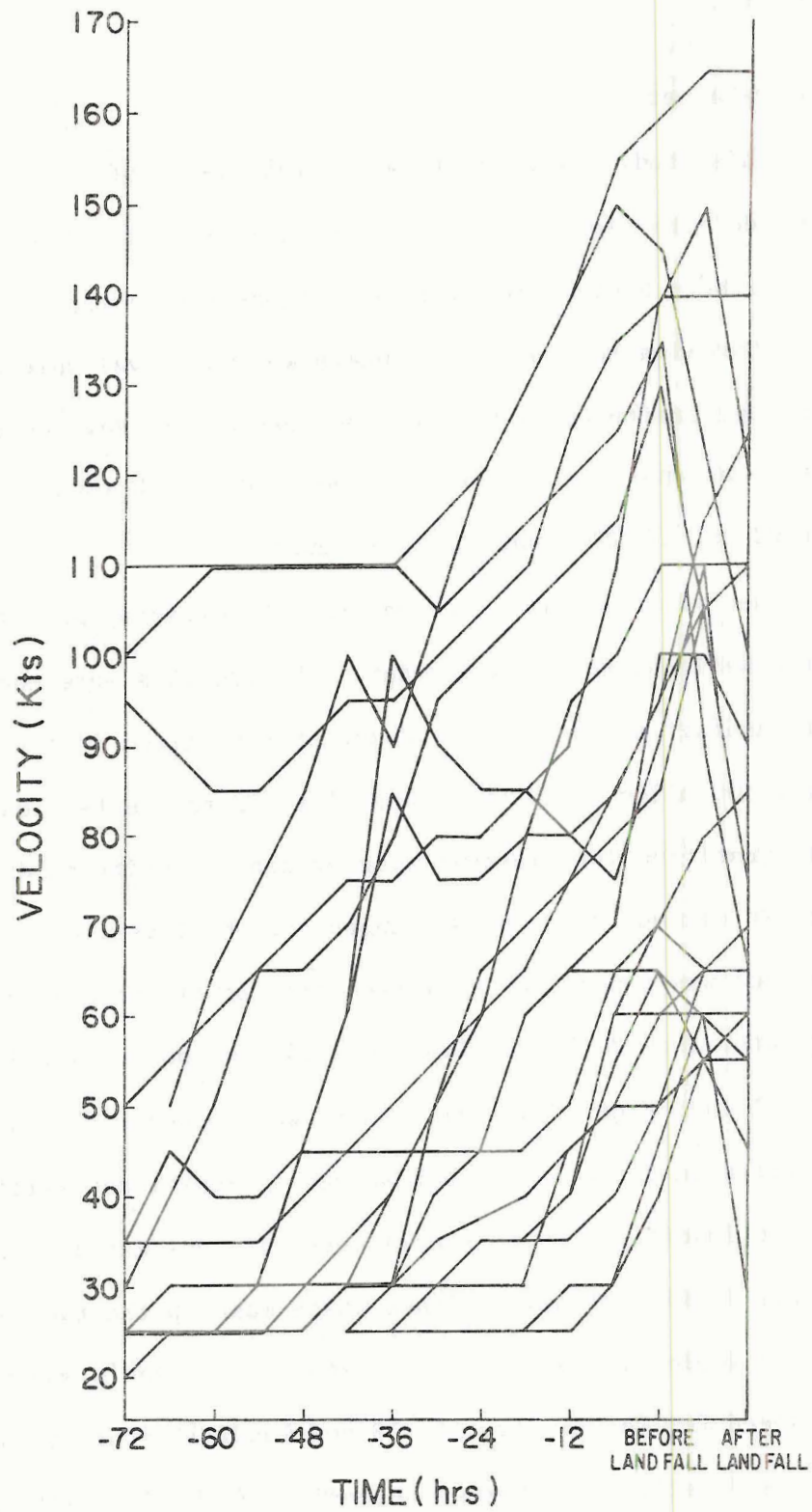


Fig. 3. Wind speed changes for all storms which make up the intensifying composite data set.

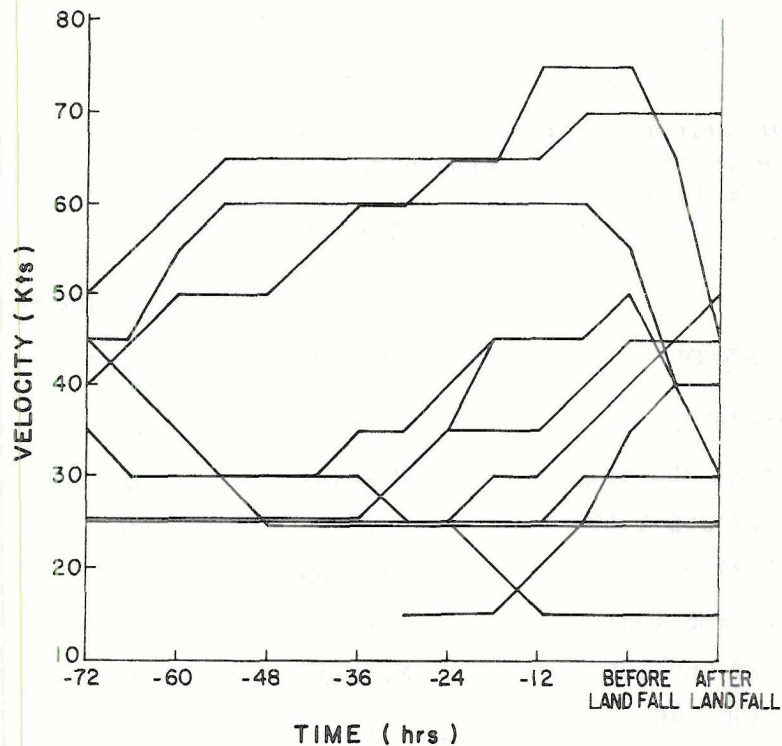


Fig. 4. Maximum wind speed changes for all storms which make up the non-intensifying composite data set.

The composites were prepared for two time periods - approximately 18 and 42 hours prior to the landfall period. These time periods were selected to approximate the critical warning periods used by the National Hurricane Center (i.e., 24 and 48 hours prior to landfall). The landfall period minus 18 hours (LF -18) was obtained by using both the LF -12 and LF -24 data composited around the LF -18 cyclone position. This was done to double the rawinsonde reports because the data samples were small (22 intensifying cases vs. 13 non-intensifying cases). Similarly, the LF -42 composite was obtained by using LF -36 and LF -48 data. The number of soundings which fell into each of the 64 grid boxes for the period LF -18 is shown in Fig. 5 for the intensifying and non-intensifying sets. It is easy to see from this figure that the most abundant data sources lie to the poleward side of the storm - a factor which we will take into consideration later. The distribution of soundings for

TABLE 1

Listing of individual storms for the intensifying and non-intensifying composite sets relative to time before Landfall (LF). The maximum sustained wind (in knots) is indicated for the three time periods.

<u>INTENSIFYING SET</u>			
<u>MEASURED OR ESTIMATED MAXIMUM SUSTAINED WIND (kts)</u>			
<u>STORM</u>	<u>LF -42</u>	<u>LF -18</u>	<u>LF</u>
H <sup>1</sup> Audry 25-28 JUN 1957	60	80	125
T <sup>2</sup> Bertha 8-11 AUG 1957	Missing <sup>3</sup>	35	60
H Debra 22-27 JUL 1959	25	35	70
H Judith 17-21 OCT 1959	Missing	30	65
H Carla 3-15 SEP 1961	110	130	150
H Cindy 16-19 SEP 1963	Missing	30	70
T Abby 5-8 AUG 1964	25	25	55
H Isbell 8-16 OCT 1964	30	80	110
H Betsy 26 AUG - 12 SEP 1965	110	115	135
H Beulah 5-22 SEP 1967	95	110	140
H Abby 1-13 JUN 1968	30	60	65
T Candy 22-26 JUN 1968	Missing	25	60
H Camille 14-22 AUG 1969	100	130	165
H Celia 30 JUL - 5 AUG 1970	60	85	110
H Ella 8-13 SEP 1970	30	70	110
T Felice 11-17 SEP 1970	30	30	60
H Edith 5-18 SEP 1971	45	45	85
H Carmen 29 AUG - 10 SEP 1974	70	105	130
H Caroline 24 AUG - 1 SEP 1975	35	65	100
H Eloise 13-24 SEP 1975	45	65	110
H Anita 29 AUG - 2 SEP 1977	75	85	150
H Babe 3-8 SEP 1977	25	40	65
-----			
AVERAGE INTENSITY	56	67	100
-----			
AVERAGE CHANGE OF MAXIMUM SUSTAINED WIND SPEED		11	33

TABLE 1 (cont'd)

NON-INTENSIFYING SETMEASURED OR ESTIMATED MAXIMUM SUSTAINED WIND (kts)

<u>STORM</u>	<u>LF -42</u>	<u>LF -18</u>	<u>LF</u>
T Debbie 7-8 SEP 1957	Missing	35	35
T Esther 16-19 SEP 1957	Missing	45	45
H Ella 30 AUG - 6 SEP 1958	60	60	55
T Arlene 28 MAY - 2 JUN 1959	30	45	50
T Irene 6-8 OCT 1959	Missing	30	50
T TS#1 <sup>4</sup> 22-26 JUN 1960	Missing	15	40
T Florence 17-26 SEP 1960	25	25	25
T TS#1 2-11 JUN 1964	25	25	30
T TS#1 11-18 JUN 1965	25	35	45
H Gladys 13-21 OCT 1968	65	65	70
T Genny 1-6 OCT 1969	25	25	25
H Alma 17-27 MAY 1970	30	25	25
H Agnes 14-22 JUN 1972	55	65	75
-----			
AVERAGE INTENSITY	38	38	44
-----			
AVERAGE CHANGE OF MAXIMUM SUSTAINED WIND SPEED		0	6
-----			

<sup>1</sup>H represents a maximum intensity of hurricane ( $\geq$  65 kts).

<sup>2</sup>T represents a maximum intensity of tropical storm ( $\geq$  35 kts)

<sup>3</sup>Missing is used because the cyclone had not yet formed.

<sup>4</sup>TS#1 of 1960 should have been stratified as an intensifying system based on post analysis. The error could not be corrected for the composite study but the system is treated as an intensifying cyclone in sections 3 and 5.



the LF -42 time period was similar to that shown for the time period LF -18.

## 2. RAWINSONDE COMPOSITE COMPARISON: INTENSIFYING VS. NON-INTENSIFYING

Although meteorological parameter comparisons between the intensifying and non-intensifying composite data sets were made for the inner 0-4° radial belts, the most reliable comparisons are found at outer radii (5-11°) where rawinsonde data is more abundant and reliable. It is also this outer 5-11° radius region which best specifies the future 1-2 day change in intensity. Also, because the intensifying data set has an average intensity which is nearly twice as large as the non-intensifying set, the differences in parameters at close radii may be biased by this intensity difference. It was observed that at outer radii the differences in cyclone intensity between the two systems is negligible. The outer region is also where we would expect any baroclinic interaction to be most noticeable. For these reasons then the main emphasis will be put on parameter differences found over outer radii (5-11°). This section examines the climatological differences, effects of movement, thermodynamic differences and dynamic differences for the composited data sets.

### 2.1 Climatological Differences

In the northwest Atlantic, August 5 through October 20 is climatologically the most active period for tropical cyclone development with a minor secondary maximum occurring in June<sup>1</sup>. Table 2 gives a breakdown of the occurrence by month of the cyclones which make up the composite study. If we let the 'active period' be the entire months of August, September and October we see that 82% of the intensifying and 54% of the non-intensifying cyclones occur during this period. If we consider all cyclones from this study which occur during the active period for

---

<sup>1</sup>Determined from cumulative summaries over the years 1886-1977 as found in Tropical Cyclones of the North Atlantic Ocean, 1871-1977.

TABLE 2

Monthly occurrence of all Gulf of Mexico storms during the years 1957-1977 which make up the composite study as listed in Table 1.

	MAY	JUN	JUL	AUG	SEP	OCT	TOTAL
INTENSIFYING	0	3	1	5	11	2	22
NON-INTENSIFYING	2	4	0	0	4	3	13

the years 1957-1977, we find that 72% of them are intensifying systems. Of all cyclones which occur during May, June or July only 40% intensify.

Preliminary inspection of Table 2 may lead to the conclusion that the basic difference between the intensifying and non-intensifying systems results from their date of occurrence. This is not the case however. Seasonal climatological differences do occur but they are not dominant. A discussion of those differences will be included in section 4. Allowances for these seasonal differences will be made as the forecasting scheme is developed.

## 2.2 Cyclone Movement

The cyclone tracks for both data sets are shown in Figs. 6 and 7. These figures indicate that, in general, cyclones with a west northwest (WNW) track are more likely to intensify while those with a north or northeast (NNE) track are more likely to fill. The average direction of movement from the composite study is towards  $303^{\circ}$  for the intensifying data set and towards  $330^{\circ}$  for the non-intensifying set at the LF -42 time period. Averages for the LF -18 time period are  $315^{\circ}$  for the intensifying set and  $342^{\circ}$  for the non-intensifying set. The differences between the data sets is a consistent  $27^{\circ}$  for both time periods.

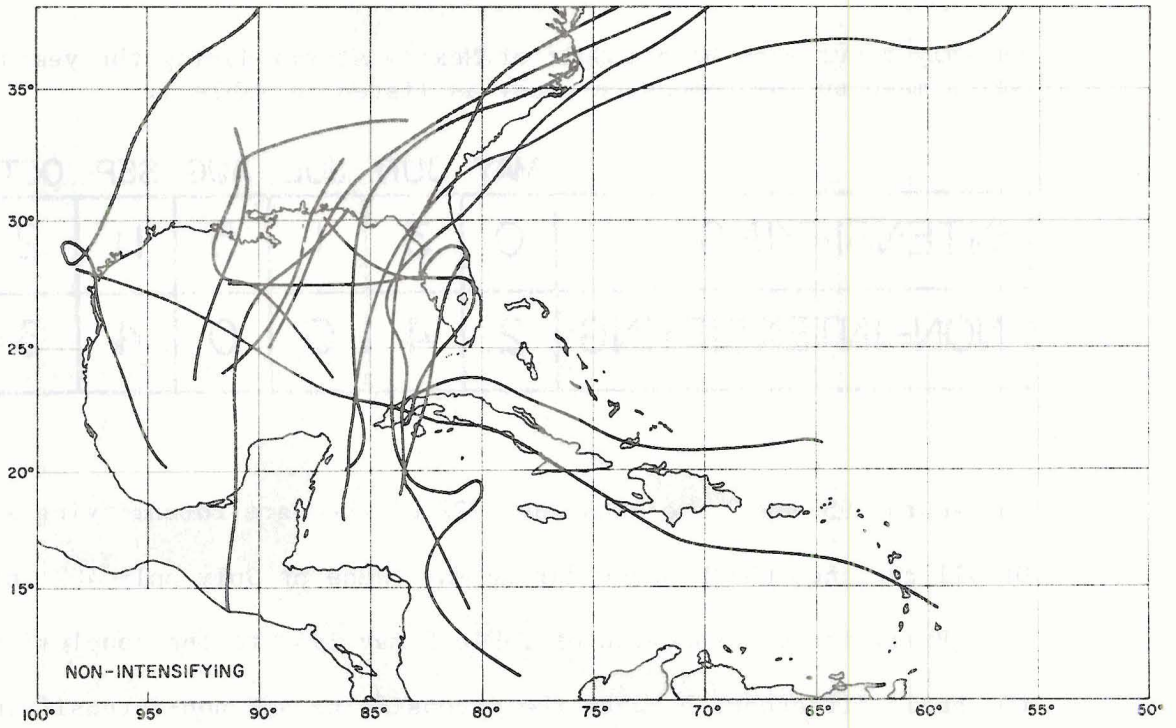


Fig. 6. Tracks of non-intensifying cyclone systems.

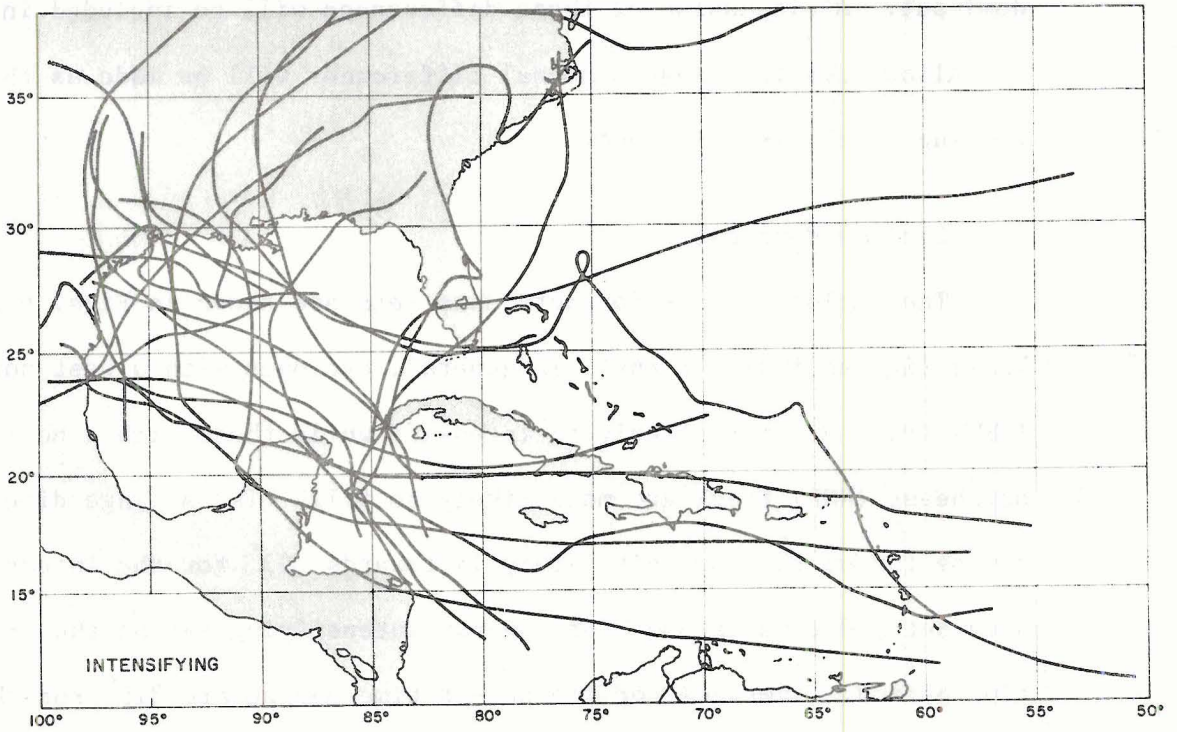


Fig. 7. Tracks of intensifying cyclone systems.

However, because of erratic cyclone movements in both data sets, any generalizations about intensity change and motion relationships may not hold well for the individual case.

The speed of movement between the two data sets was also analyzed and compared. In the mean there was little difference. But after a cyclone has made a turn toward the NNE there is a slight acceleration as the cyclone becomes caught up in the westerly wind zone. A correlation could not be found between the rate of deepening or filling and the speed of movement.

### 2.3 Thermodynamic Parameters

Temperature Differences. Figure 8 shows the 3-5° radial belt average of the vertical profile of the temperature difference obtained by subtracting the non-intensifying temperature profile from the intensifying profile at both the LF -42 and LF -18 time periods. For both time periods the intensifying set is slightly warmer through the troposphere with the largest differences occurring in the lowest levels. At the tropopause level the intensifying set is colder by one to two degrees. These differences could be due to the different average intensities between the data sets but investigation of the temperature fields at the lowest standard level (i.e., 850 mb) shows this is not so

The 850 mb temperature fields for both intensity classes at the LF -42 and LF -18 time periods are shown in Figs. 9 and 10. Diagram c of Figs. 9 and 10 represents the difference between the two data sets found by subtracting the non-intensifying data set from the intensifying set. The largest differences occur over the north and northwest quadrants of the storm. In this area the intensifying set averages two to three degrees warmer for both time periods. The analysis also shows a

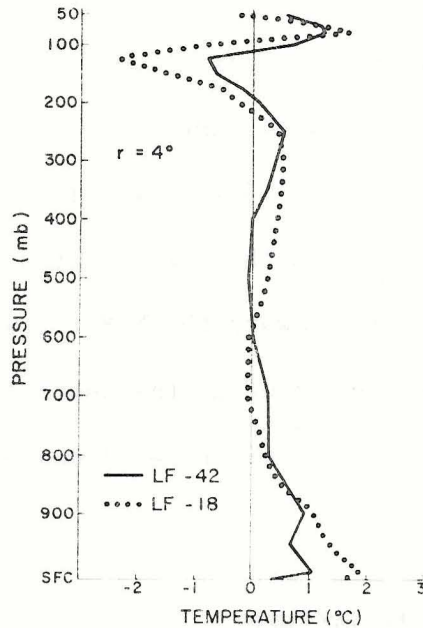


Fig. 8.  $3-5^{\circ}$  radial belt average of the vertical profile of the temperature difference obtained by subtracting the non-intensifying temperature profile from the intensifying profile at both the LF -42 and LF -18 time periods.

temperature trough over the northwest sector for the non-intensifying set - a feature not found on the intensifying maps.

Moisture Differences. Figure 11 shows the  $3-5^{\circ}$  belt average of specific humidity for the LF -18 time period and Fig. 12 is the relative humidity profile for the same time and area. The specific and relative humidities are both slightly larger for the intensifying data set but the difference is so small that it is hardly measurable. Similar comparisons for the LF -42 time period also indicate little or no difference between the two systems. This finding was also observed by Núñez (1981).

Height Differences. Because of the warmer troposphere found in the intensifying data set, the hydrostatic pressure relationships dictate that the pressure-height fields at upper levels should be higher in the intensifying set. The 200 mb height analysis is shown in Figs.

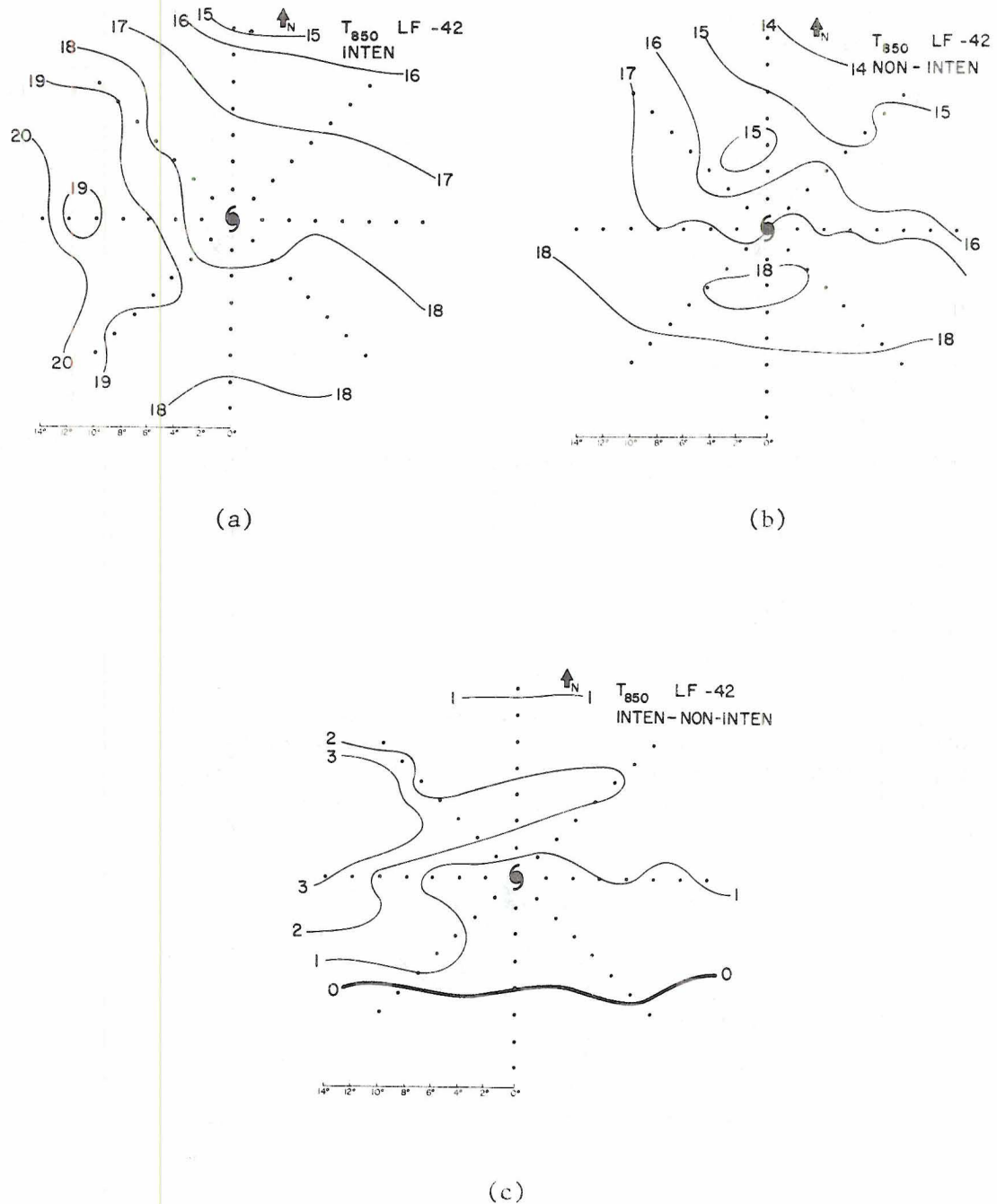


Fig. 9. 850 mb temperature field for the LF -42 time period for the intensifying data set (diagram a), the non-intensifying data set (diagram b) and the difference between the two (diagram c) obtained by subtracting the non-intensifying from the intensifying data set. Units are  $^{\circ}\text{C}$ .

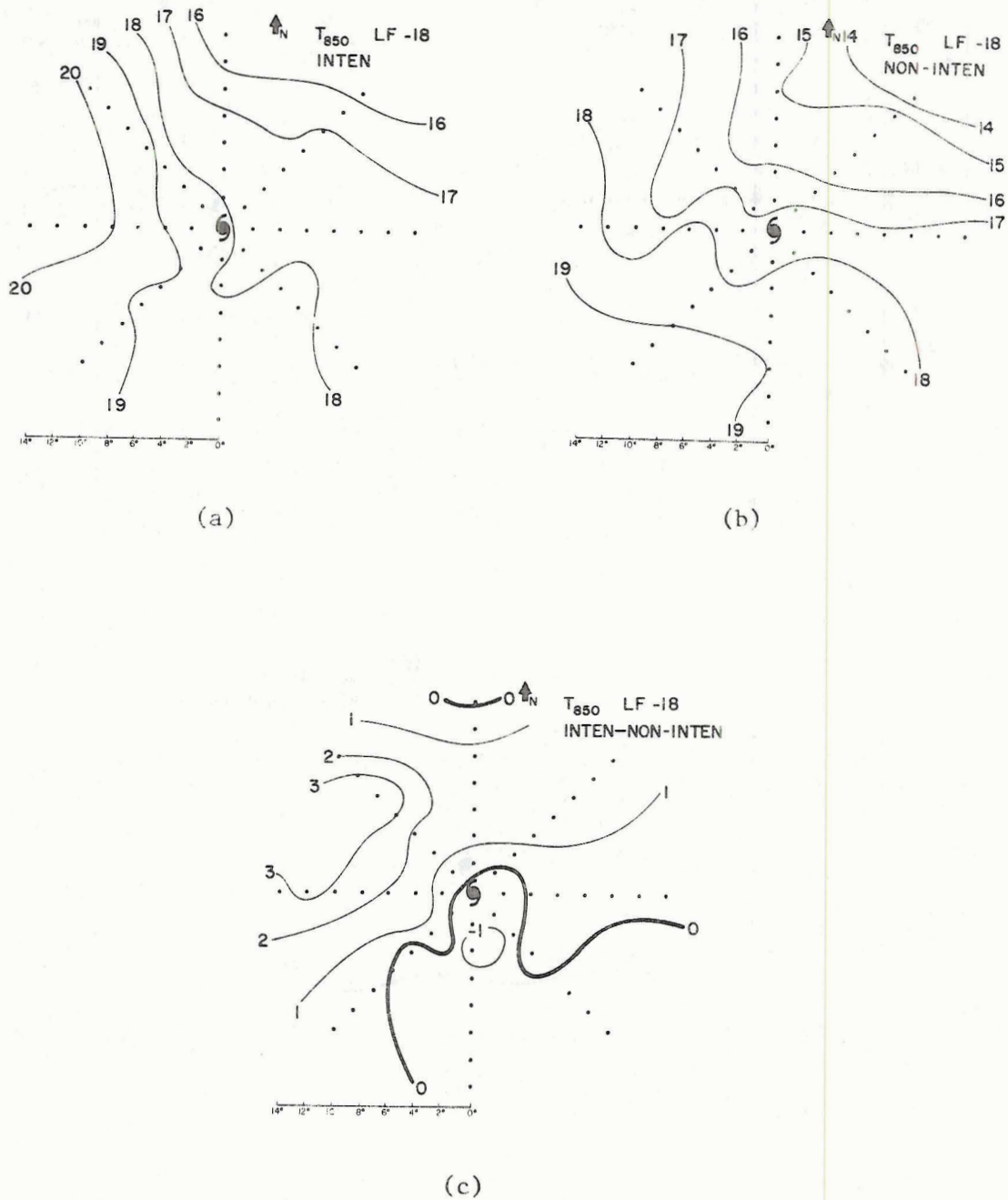


Fig. 10. Same as Fig. 9 but for the LF -18 time period.

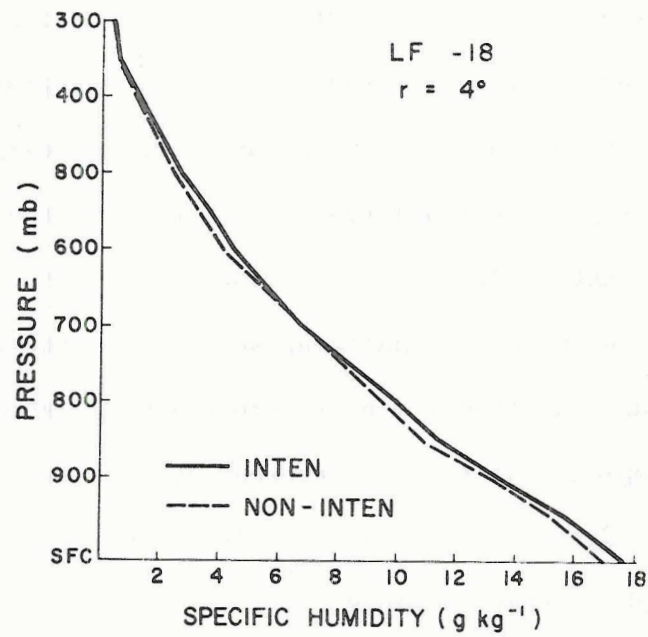


Fig. 11. The 3-5° radial belt average of specific humidity for the LF -18 time period.

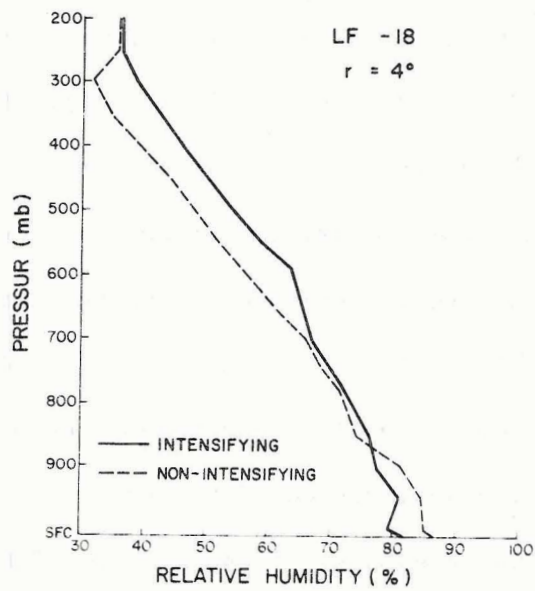


Fig. 12. The 3-5° radial belt average of relative humidity for the LF -18 time period.

13 and 14. At the LF -42 time period (Fig. 13) the anticyclone center is established in both sets but the height gradient to the north is much stronger in the non-intensifying set. Diagram c of Fig. 13 (obtained by subtracting the non-intensifying composite from the intensifying composite) shows a large difference over the west, northwest, and northern octants. At the LF -18 time period (Fig. 14), there is very little change in the intensifying set. The anticyclone center found on the previous non-intensifying figure has diminished and the presence of a trough impingement to the northwest is more evident. Again the differencing diagram (Fig. 14c) shows large height differences over the west through northern octants.

Negligible differences were found in all other thermodynamic parameters.

#### 2.4 Dynamic Differences

Total Wind. The total winds are depicted in the plan views shown in Figs. 15-18 for the 900 and 200 mb levels and for both time periods. Differences in the total winds at the 900 mb level are small for both time periods. But at 200 mb one can see that the westerlies are much stronger and extend further south in the non-intensifying set. There also is an apparent wind maximum between  $3-11^{\circ}$  on the north side. The anticyclone is not well developed in the non-intensifying set and is displaced about  $4^{\circ}$  to the southeast at the LF -42 time period. By the LF -18 time period the anticyclone becomes even more disorganized and a quick streamline analysis would put the center at about  $6^{\circ}$  to the southeast. As was previously found with the 200 mb height field, the largest differences occur over the west through north octants.

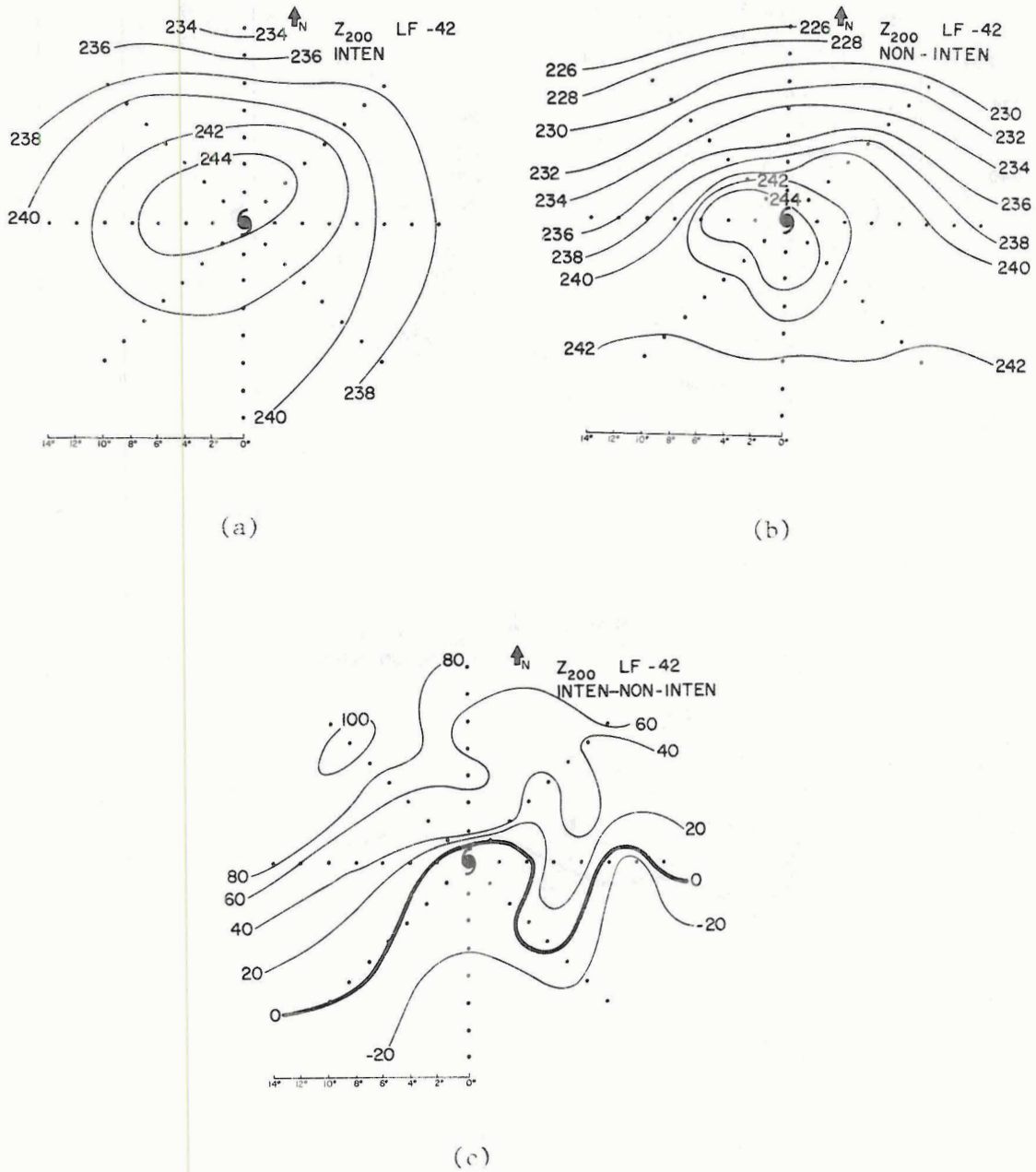
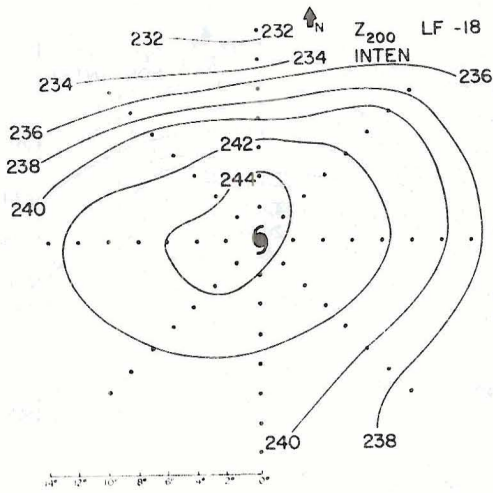
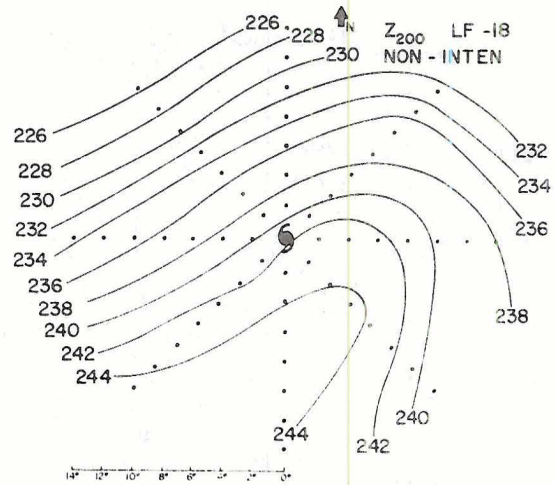


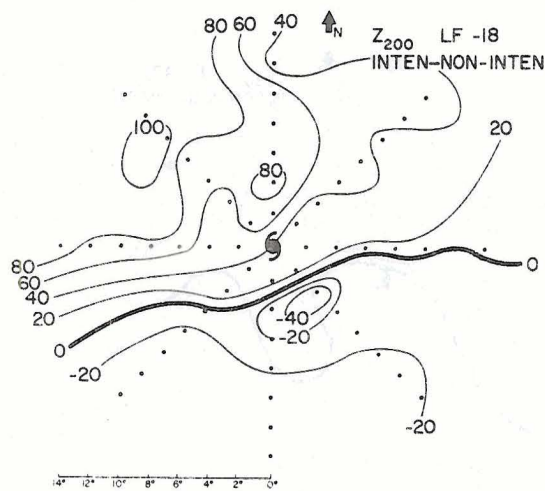
Fig. 13. LF -42 hour 200 mb height patterns for the intensifying composite (diagram a), the non-intensifying composite (diagram b) and the difference between the two (diagram c) obtained by subtracting the non-intensifying composite from the intensifying composite. Units in diagram c are meters.



(a)



(b)



(c)

Fig. 14. Same as Fig. 13 but for the LF -18 time period.

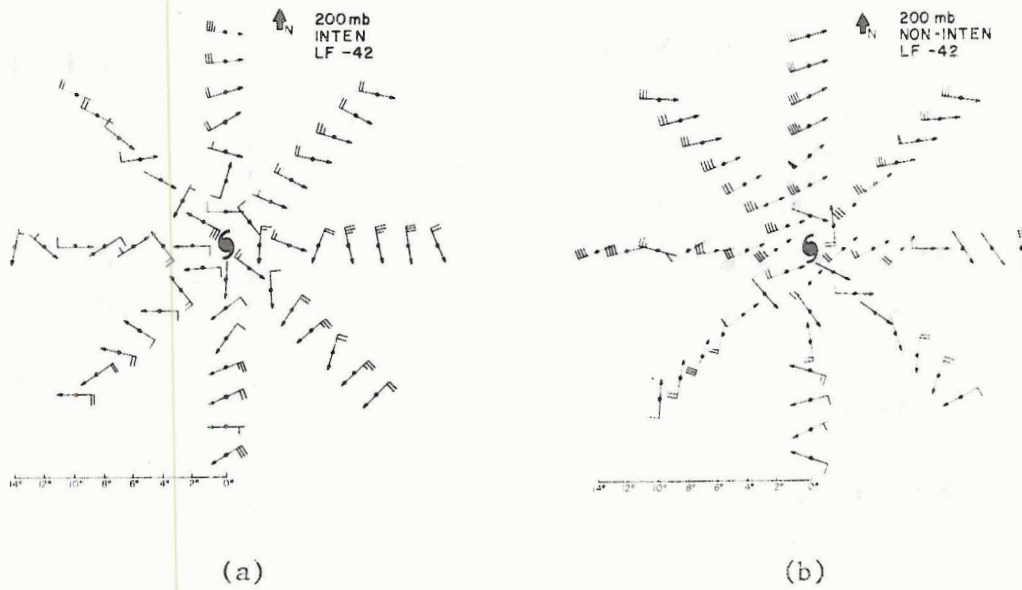


Fig. 15. Plan views of the 200 mb total winds for the intensifying data set (diagram a) and the non-intensifying data set (diagram b) for the LF -42 time period. Wind barbs are in knots where a full barb = 10 kts or  $5 \text{ m s}^{-1}$ .

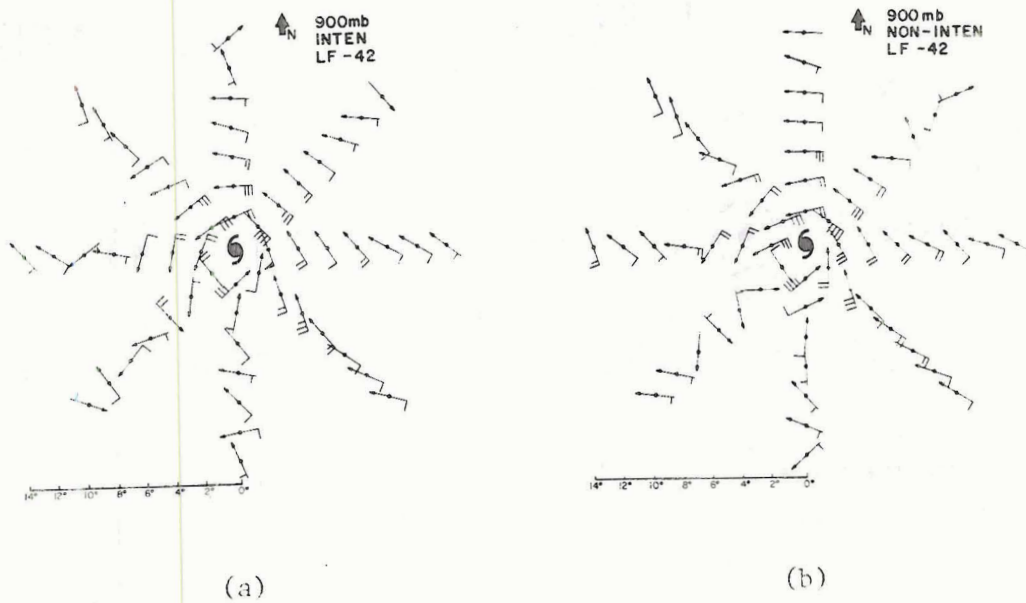


Fig. 16. Same as Fig. 15 but for the 900 mb level.

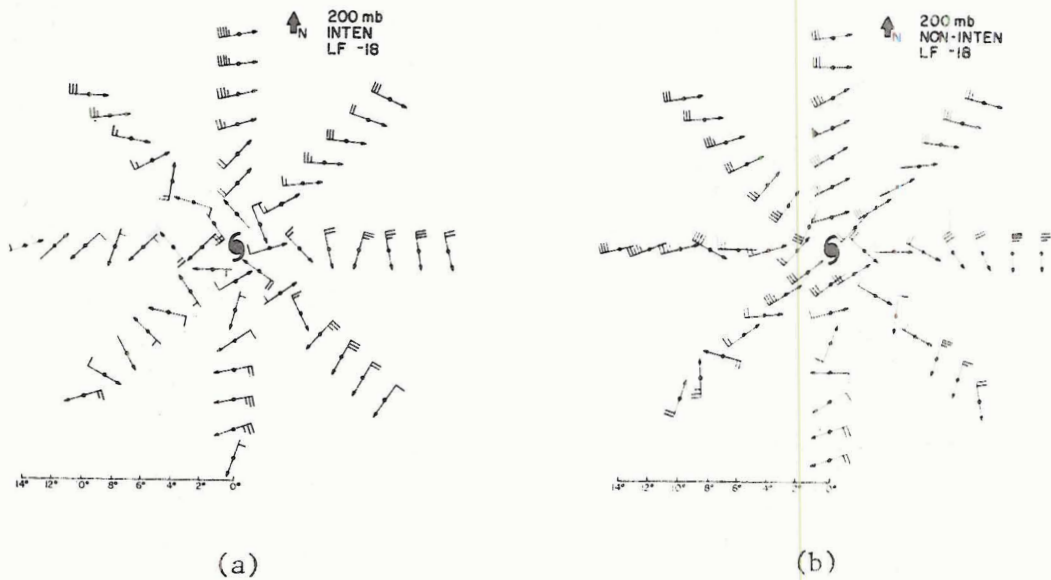


Fig. 17. Plan views of the 200 mb total winds for the intensifying data set (diagram a) and the non-intensifying data set (diagram b) for the LF -18 time period. Wind barbs are in knots where a full barb = 10 kts or  $5 \text{ m s}^{-1}$ .

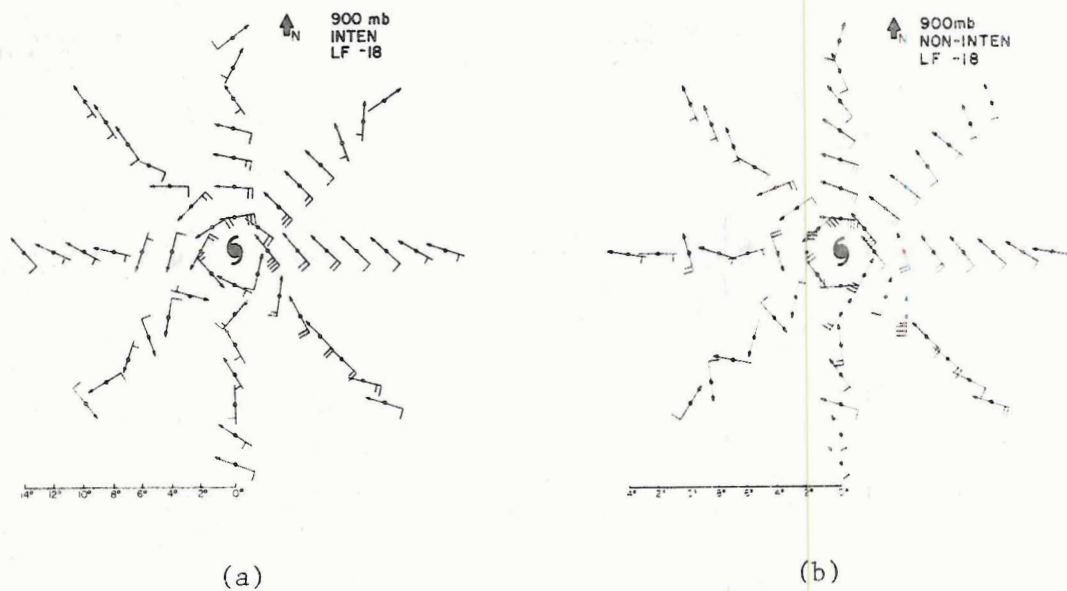


Fig. 18. Same as Fig. 17 but for the 900 mb level.

Zonal Winds. The zonal wind at 200 mb was next investigated and the results can be seen in Figs. 19 and 20. Again the major differences occur to the west and north but the zonal wind also shows some major differences in the southwest octant providing more evidence of a trough intrusion. The 200 mb wind maximum found in the plan views of the total winds (Figs. 15b and 17b) appears to be more confined to the 5-11° belt on the north side. This wind maximum has a strength of 20-24 m s<sup>-1</sup> and is a persistent feature between the two time periods.

Vertical Wind Shear. Another feature which has been found by other investigators (Gray, 1968, 1975; McBride, 1979) and which is also apparent in this data set is the presence of weak vertical wind shear near the center of the intensifying system. Figures 21 and 22 show the plan views of the mean shear of the zonal wind,  $U_{200 \text{ mb}} - U_{900 \text{ mb}}$  for the two time periods. At both time periods the intensifying set maintains the zero shear line over the top of the storm while the non-intensifying set has 15-20 m s<sup>-1</sup> shear above storm center. McBride (1979) indicated the need for strong upper tropospheric westerly shear to the poleward side and strong easterly shear to the equatorward side for cyclone development. This phenomenon is present in the intensifying data set at both the LF -42 and LF -18 time periods. The non-intensifying data set also has a large westerly shear to the north but closer analysis reveals that the middle level baroclinicity (i.e. 850-400 mb) contributes largely to the shear. In contrast, the majority of the shear found in the intensifying set comes from the upper troposphere (i.e. 350-200 mb). Also, the non-intensifying data set does not exhibit easterly shear to the south until reaching large radii.

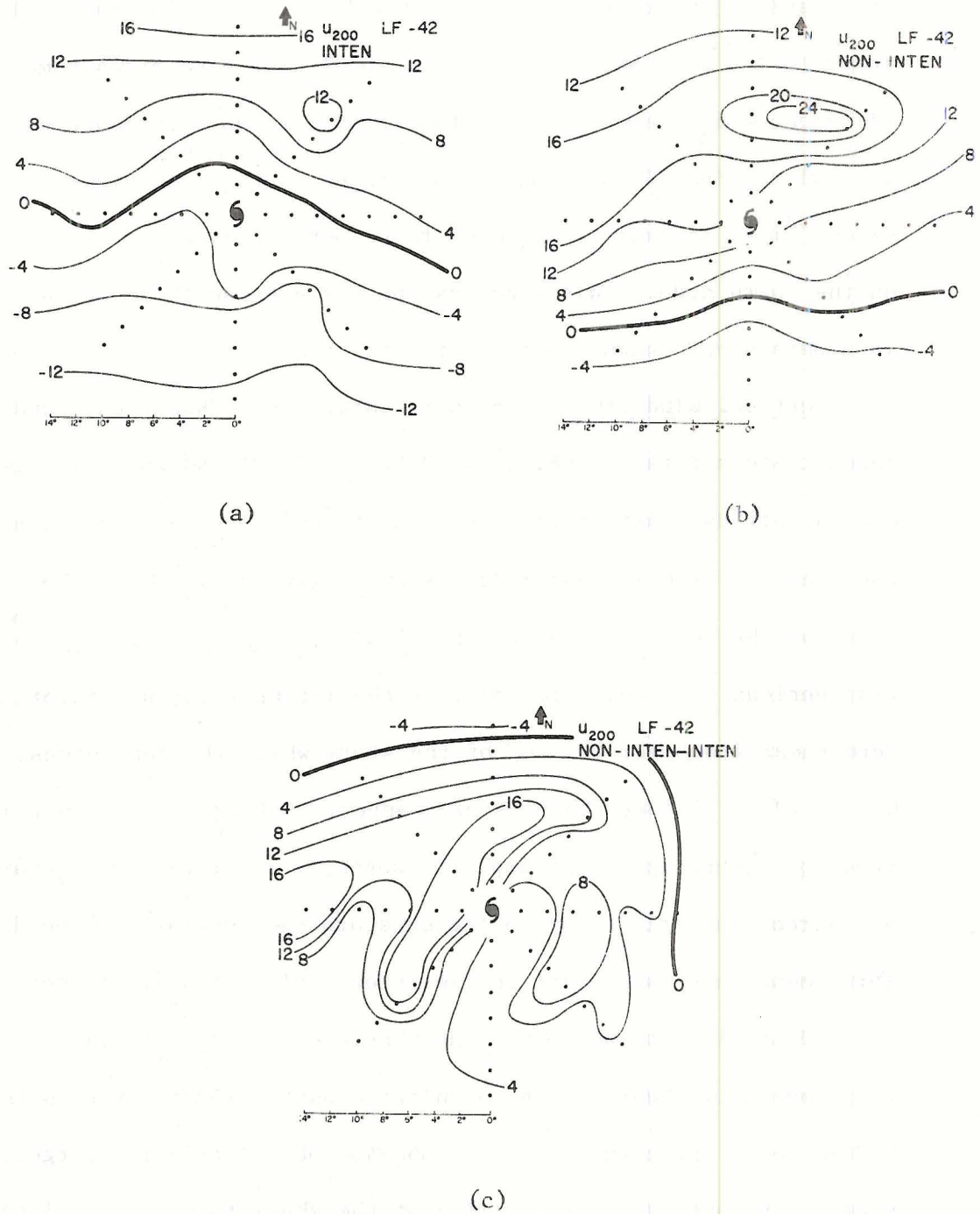
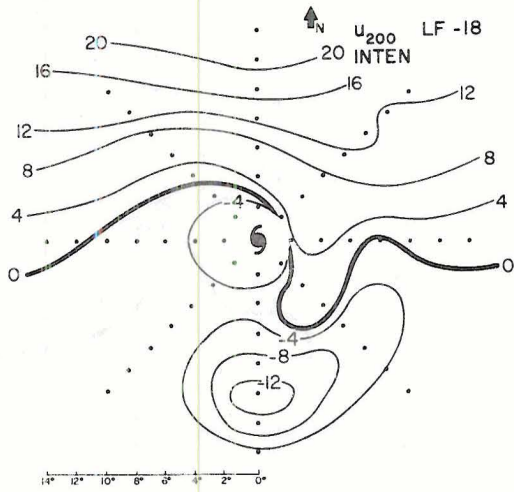
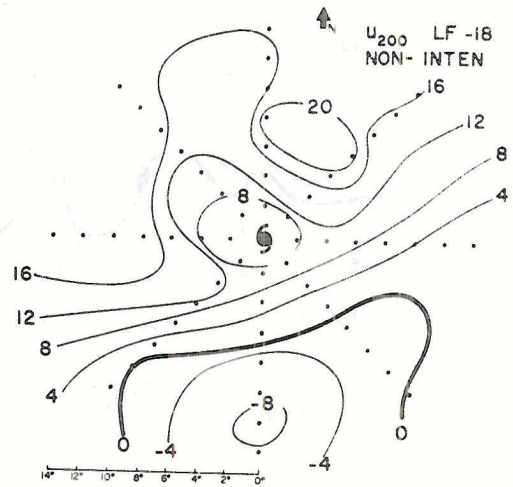


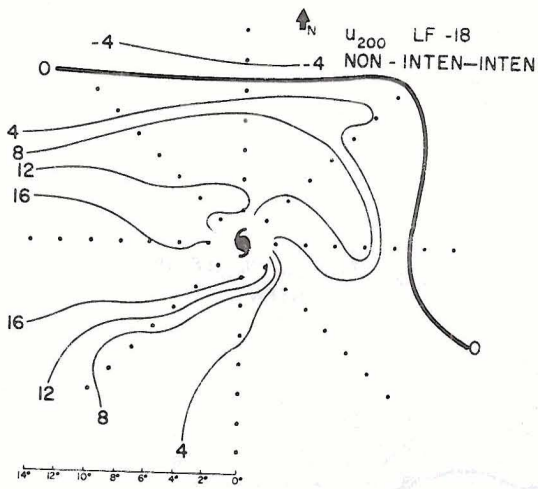
Fig. 19. 200 mb zonal wind field for the LF -42 time period for the intensifying data set (diagram a), the non-intensifying data set (diagram b) and the difference between the two (diagram c) found by subtracting the intensifying data set from the non-intensifying data set. In diagram c positive numbers indicate that the zonal wind is stronger in the non-intensifying data set. Units are  $\text{m s}^{-1}$ .



(a)



(b)



(c)

Fig. 20. Same as Fig. 19 but for the LF -18 time period.

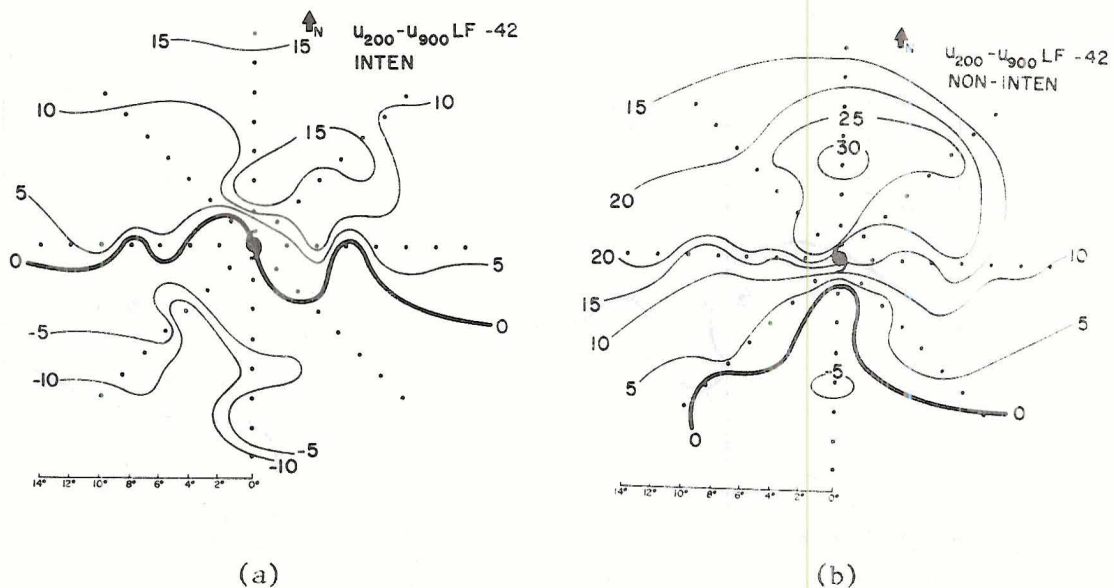


Fig. 21. Plan views of the zonal wind shear ( $U_{200 \text{ mb}} - U_{900 \text{ mb}}$ ) (in units of  $\text{m s}^{-1}$ ) for the intensifying data set (diagram a) and the non-intensifying data set (diagram b) for the LF -42 time period.

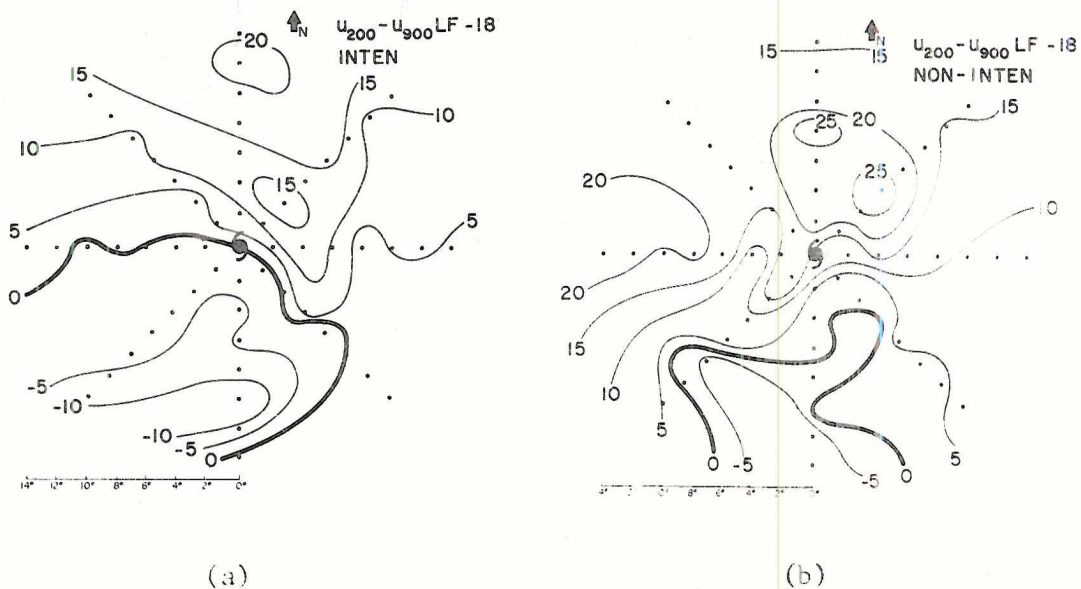


Fig. 22. Same as Fig. 21 but for the LF -18 time period.

The radial wind, tangential wind, divergence and vertical motion parameters were closely examined for both data sets. The differences noted were that the intensifying systems maintained an inflow through a deeper layer resulting in more convergence and stronger vertical motion than observed in the non-intensifying systems. Because of the difficulty in calculating the parameters on an individual case basis, these parameters will not be considered for further investigation.

## 2.5 Summary of Composite Results

The composite results show that large differences occur in specific meteorological parameters between intensifying and non-intensifying tropical cyclone systems. It appears that these differences are a result of large scale baroclinic interaction since most of the differences were found on the poleward side of the storm. The major results of the composite study are:

- 1) The large scale environment of the intensifying cyclone is warmer through the depth of the troposphere with the largest differences found below 700 mb. The horizontal plan views at 850 mb indicate that most of the temperature difference occurs over the west through north octants.
- 2) Moisture analysis is not a good indicator of intensification.
- 3) The largest height differences occur at the upper levels over the west through north octants. The horizontal height gradients are also strongest to the north and northwest.
- 4) The westerlies extend further south and are much stronger in the non-intensifying set. A small wind maximum occurs between  $5^{\circ}$  and  $11^{\circ}$  on the poleward side of the non-intensifying system.
- 5) The differences in the zonal wind are largest over the southwest to north octants. This yields evidence of a baroclinic trough impinging upon the non-intensifying system from the west.
- 6) An area of zero vertical zonal wind shear  $U_{200 \text{ mb}} - U_{900 \text{ mb}}$  exists over the center of the intensifying set while  $15\text{-}20 \text{ m s}^{-1}$  shear is found just to the west and east of the non-intensifying storm center.

### 3. DEVELOPMENT OF THE INTENSITY CHANGE FORECASTING SCHEME

The results of the composite study indicated important parameter differences on the northwest side of the cyclone systems. Therefore, this study chose to concentrate on the region between 5 and 11° over octants 8, 1 and 2. For cyclones moving through the Gulf of Mexico, this region gives the best data coverage (see Fig. 23).

Results derived from the composite analysis of the previous section were applied to individual cases of the composite data sets. This was done to see how well the composite information could be used on an individual case basis. Additionally, it gives us a quantitative measure for how applicable a forecasting scheme might be.

For simplicity only the standard weather charts analyzed at the 850, 500, and 200 mb levels were utilized. These charts are readily available to forecasters in any weather station and can be used to make the rapid computations necessary in an operational environment. Also, by selecting these levels we can supplement the 850 and 200 mb charts with satellite derived winds in the data sparse regions.

#### 3.1 Selection of Parameters

Temperature. The composite results indicated that the 850 mb temperature field was noticeably different over the northwest octant of the intensifying vs. non-intensifying storm system. The 850 mb temperature was selected as one of the parameters and an average value was computed over the octants 8, 1 and 2 within the 5-11° radial belt through linear averaging by 2° radial belts. Applying this procedure to the two data sets at both time periods yielded an average 850 mb

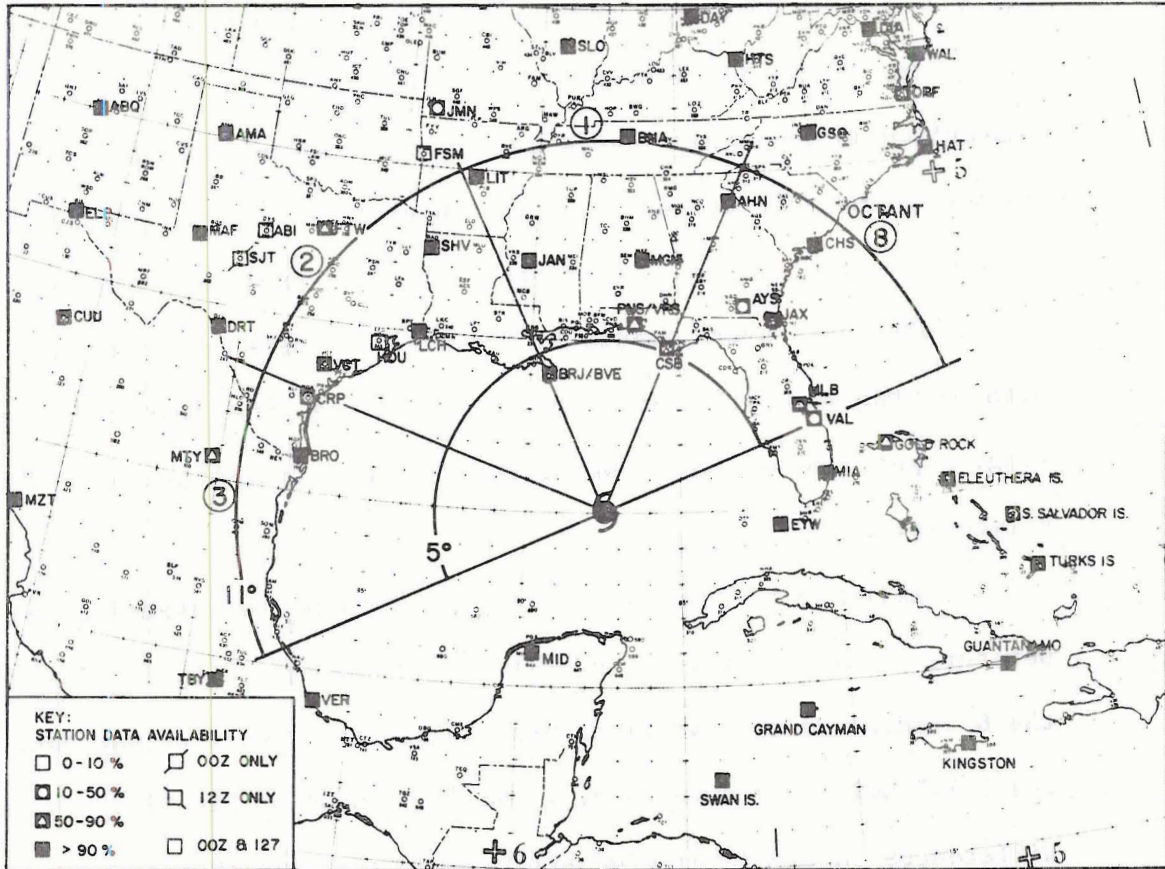


Fig. 23. Example of the distribution of rawinsonde stations for the Gulf of Mexico region. Notice the lack of data from the southeast to west Gulf regions.

temperature of  $17.5^{\circ}\text{C}$  for the intensifying data set vs.  $15.5^{\circ}\text{C}$  for the non-intensifying data set or a difference of  $2^{\circ}\text{C}$ .

Height. The 200 mb height differences between the intensifying and non-intensifying data sets computed over the  $5-11^{\circ}$  radial belt over octants 8, 1 and 2 was about 60 m for both the LF -42 and LF -18 time periods. Heights were 12410 m for the intensifying set and 12350 m for the non-intensifying set. The  $5-11^{\circ}$  radius horizontal height gradients were analyzed but the differences between the data sets was only about 12 m per  $6^{\circ}$  radius.

Zonal Wind. Large differences were noted earlier in the zonal wind fields. Vertical profiles of the zonal wind were first made for

the 5-7° radial belt over the northwest sector, octants 1, 2 and 3 (Fig. 24). Very large differences occur, particularly in the strength of the westerlies in the upper levels and in the vertical shear. But for storms in the Gulf of Mexico we encountered the problem of data deficiencies over octant 3. Therefore, a similar profile was made for the 5-7° radial belt over octants 8, 1 and 2. Results are shown in Fig. 25. Although the wind differences are not as large, they are still very striking, especially at 200 mb where the differences are more than  $10 \text{ m s}^{-1}$  between systems.

Finally, to be consistent with the methods for computing the temperature and height values and also to smooth out possible eddies in the 6° radial belt, a vertical profile of the zonal wind was made for the 5-11° belt over octants 8, 1 and 2 as shown in Fig. 26. The same differences in the zonal wind still occur although they are not as large. By expanding the areal coverage of the measurement we can minimize the data noise and get a more stable representation of the parameter differences. Therefore, we will average all parameters over the 5-11° radial belt. This improves the data quality without greatly reducing the differences between the two systems.

Vertical Wind Shear. The vertical wind shears computed over the 5-11° radial belt over octants 8, 1 and 2 between 850-500 mb and 850-200 mb are also very different (Fig. 26). The 850-500 mb vertical wind shear is only about  $3 \text{ m s}^{-1}$  for the intensifying set vs.  $6 \text{ m s}^{-1}$  for the non-intensifying set. The 850-200 mb vertical shear is about  $12 \text{ m s}^{-1}$  for the intensifying set vs.  $21-25 \text{ m s}^{-1}$  for the non-intensifying data set. The differences are even larger if we compute the vertical shears from Figs. 24 and 25.

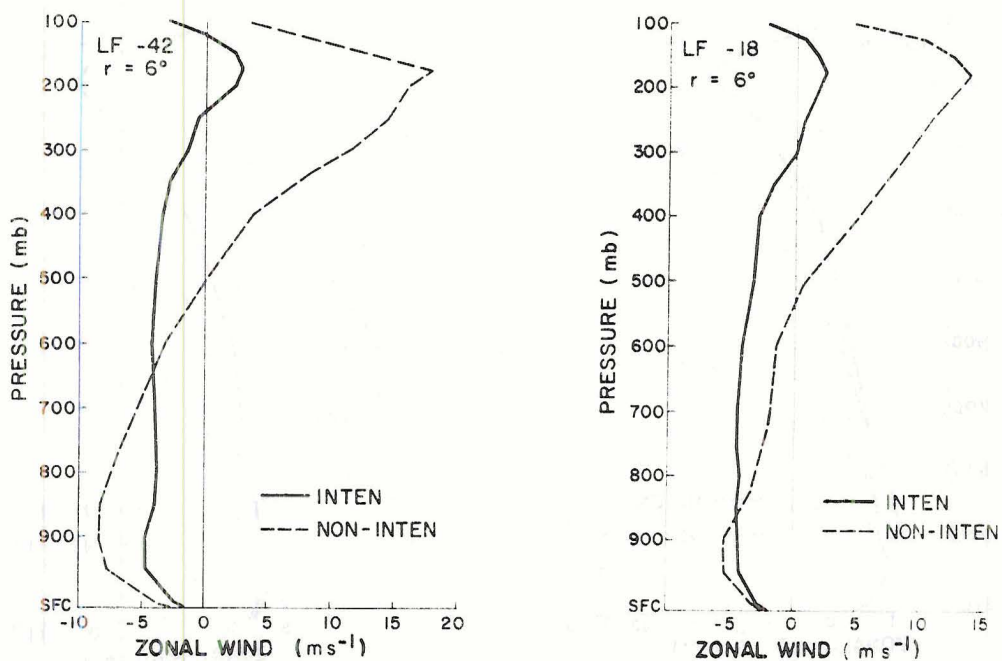


Fig. 24. The vertical profile of the zonal wind for the 6° radial belt averaged over octants 1, 2 and 3 for the LF -42 time period (left diagram) and the LF -18 time period (right diagram).

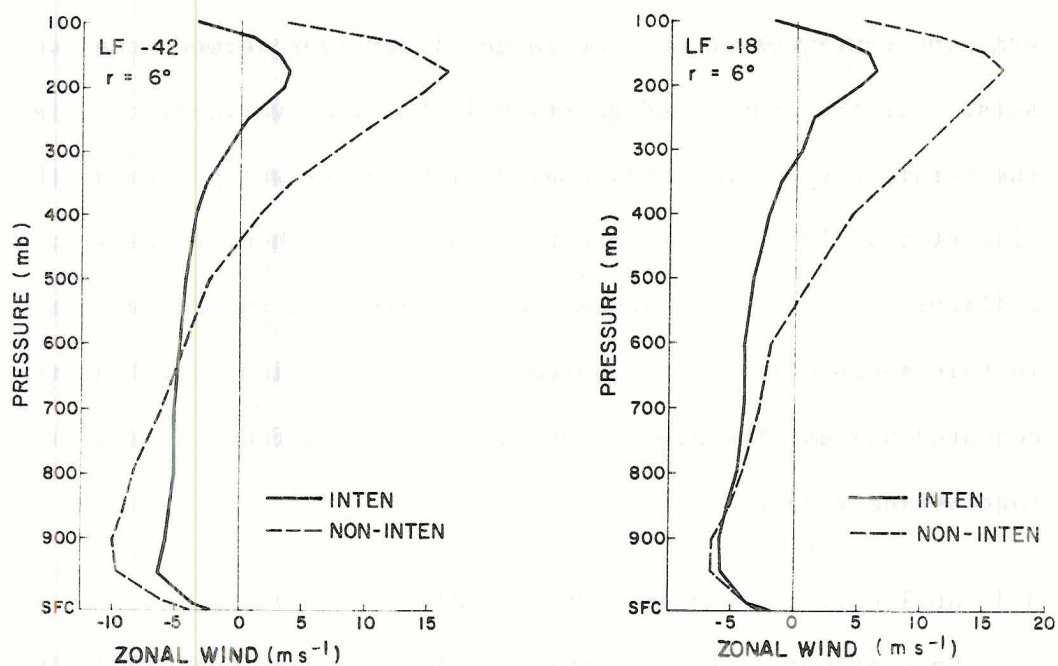


Fig. 25. The vertical profile of the zonal wind for the 6° radial belt averaged over octants 8, 1 and 2 for the LF -42 time period (left diagram) and the LF -18 time period (right diagram).

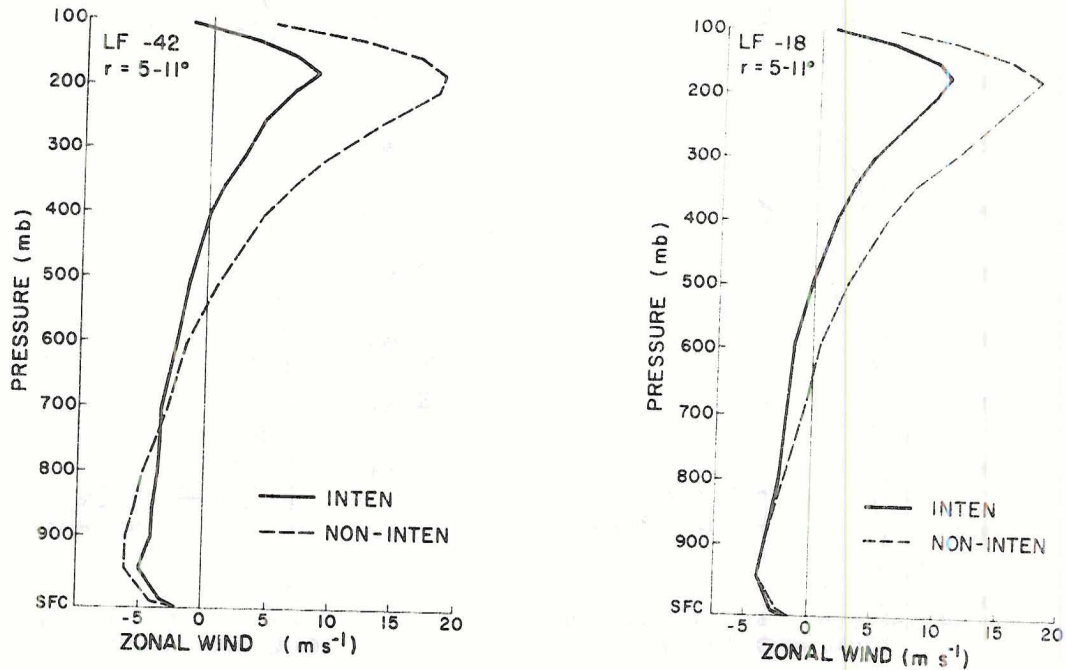


Fig. 26. The vertical profile of the zonal wind averaged over the  $5-11^{\circ}$  radial belt for octants 8, 1 and 2 for the LF -42 time (left diagram) and the LF -18 time period (right diagram).

Summary. Further analysis of the composite data sets on the northern side continues to produce large differences between the two data sets. But the unanswered question is how much variability exists in the parameters of the individual cyclone cases which make up the composite study. Furthermore, how well can we use these results to produce skillful forecasts? To answer these questions, the parameters discussed in this section will be measured for each individual cyclone system and compared against the mean to see if we can, in fact, produce a reliable forecasting scheme.

### 3.2 Application of Parameters to Individual Cases

Special computer programming techniques developed by Edwin Buzzell of the CSU tropical storm group were employed to retrieve the data for each of the individual storms which made up the composites. Objective procedures were used to calculate all parameters. In data-sparse regions

smoothing procedures were used to determine the parameter values. A complete listing of the computations can be found in Tables 7-10 of Appendix A. A summary of those tabular values can be seen in Figs. 27 and 28.

Temperature. The average 5-11<sup>o</sup> radius 850 mb temperature for all cyclones ranged from 13.5<sup>o</sup>C to 21<sup>o</sup>C. The value of 15.5<sup>o</sup>C was chosen as a threshold value upon which to base intensification. Only 9% of the intensifying systems (2 of 23 cyclones averaged over the LF -42 and LF -18 time periods) had an 850 mb temperature colder than 15.5<sup>o</sup>C. Of the non-intensifying systems, 50% (6 of 12 storms) have 850 mb temperatures warmer than 15.5<sup>o</sup>C but had other parameters which did not favor intensification. Of all cyclones averaged over the two time periods, 77% could have been identified as intensifying or non-intensifying simply from their respective 5-11<sup>o</sup> radius 850 mb temperature fields being warmer or colder than 15.5<sup>o</sup>C.

Height. The 200 mb height field averaged over the 5-11<sup>o</sup> radial belt over octants 8, 1 and 2 also displays a good delineation between systems. The value of 12380 m provided a base value upon which 74% and 80% of the storms at the LF -42 and LF -18 time periods could have been characterized as intensifying or not. Most of the remaining 26-20% was made up of intensifying systems with height values < 12380 m. In no case did a storm intensify with a height field < 12320 m and conversely only one storm did not intensify when the height field was > 12420 m. Furthermore, at the LF -18 time period as the cyclone approached landfall and further baroclinic interaction, only one cyclone did not intensify with a height field > 12380 m.

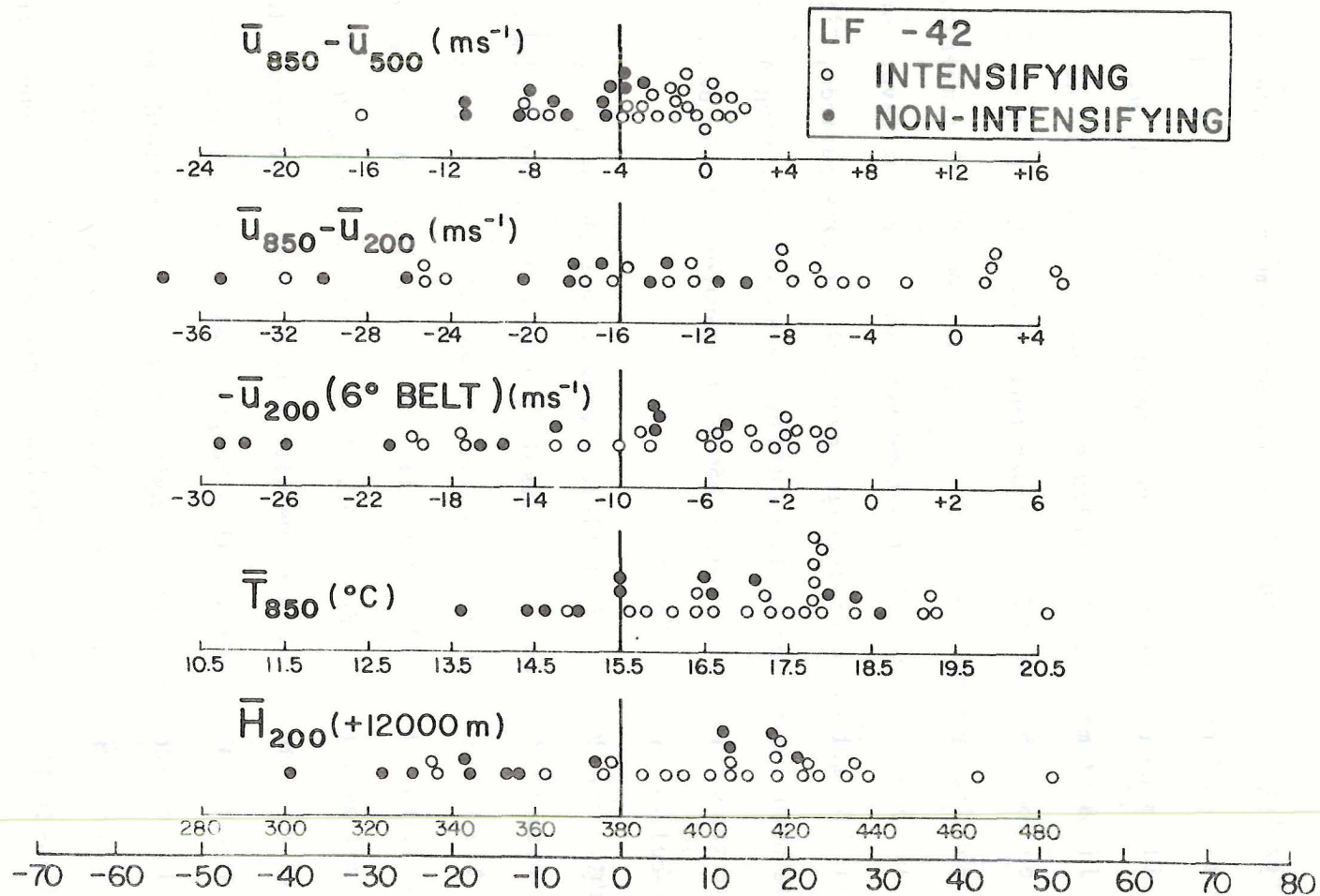


Fig. 27. Tabular values of each of the five intensity change parameters as they are distributed in their respective scatter graph for the LF -42 time period. The 0 line represents the threshold value of each parameter as determined from the scatter of the data. The abscissa on the bottom of the graph is used in the computation of the intensity change parameter.

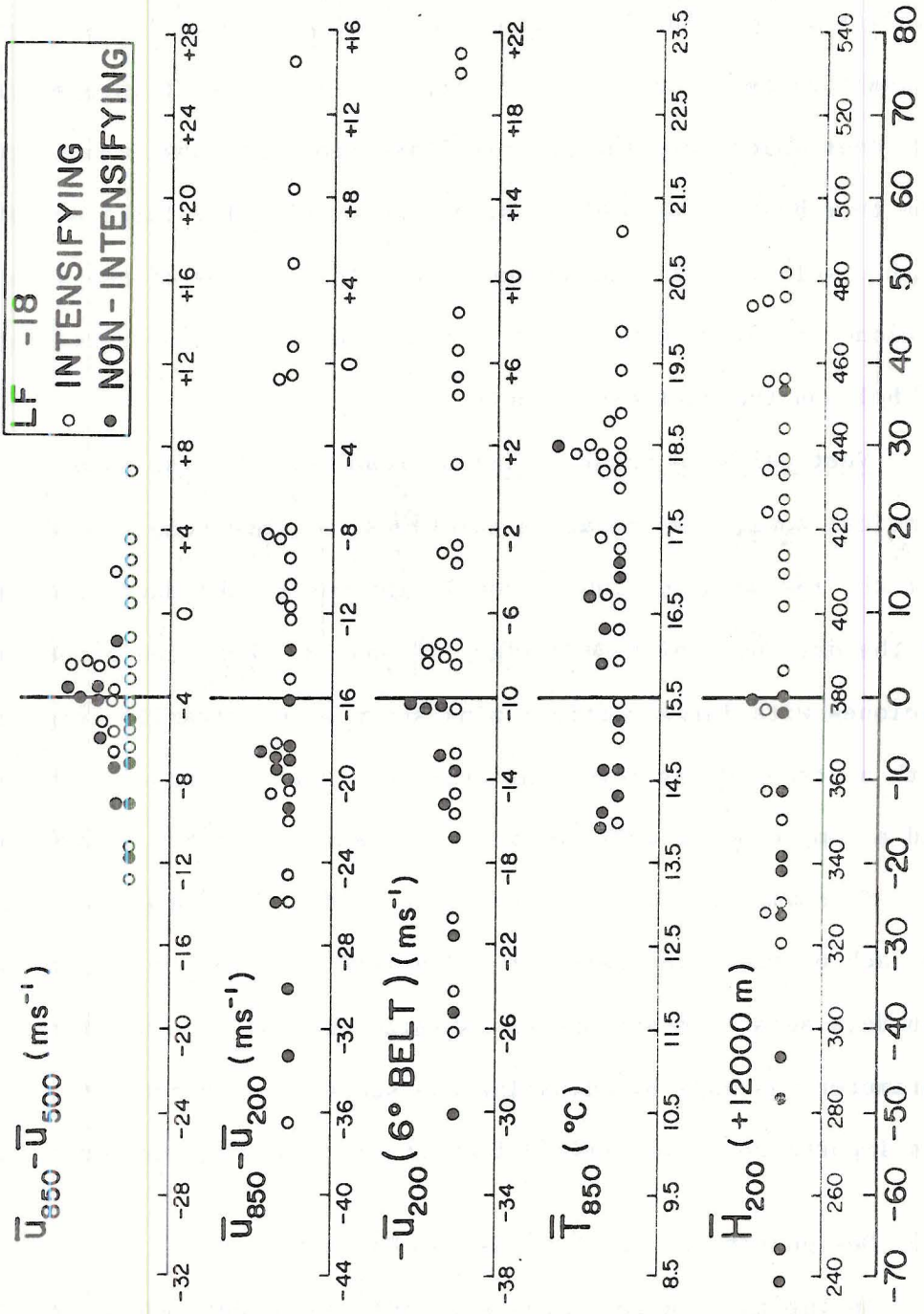


Fig. 28. Same as Fig. 27 but for the LF -18 time period.

Zonal Wind. The individual case measurements of the impinging zonal westerlies upon the storm system also verifies the results of the composites. The negative of the zonal wind ( $-\bar{U}_{200}$ ) is plotted in Figs. 27 and 28 and the established threshold is  $-10 \text{ m s}^{-1}$ . The results are best at the LF -18 time period where 80% of the cyclones are properly classified as intensifying or not. The majority of intensifying cyclones which were incorrectly classified had zonal winds stronger than the threshold value. These storms were primarily large and strong systems with a well established anticyclone. The effects of the strong anticyclone at 200 mb was to add to the strength of the westerlies in the  $6^\circ$  belt on the northern octants.

Vertical Wind Shear. Similar results were also found in the vertical zonal wind shear calculations. A threshold value of  $-16 \text{ m s}^{-1}$  for the 850 mb minus 200 mb zonal wind was established from the scatter of the data as depicted in Figs. 27 and 28. Here again the intensifying cyclones with large vertical wind shear were primarily large cyclones with a strong upper level anticyclone. However, most of these cyclones had a compensating weak vertical wind shear from 850 to 500 mb.

To summarize Figs. 27 and 28 we find that a large variability exists in each of the parameters but a distinct division is evident between the two data sets. An attempt to maximize the positive benefits of each parameter was made by adjusting the scale of each parameter based on its importance as determined from statistical methods shown in section 5.

### 3.3 Designation of the Forecasting Parameter

An intensification parameter (IP) can be determined from a normalized sum of each parameter as determined from the scale on the bottom of Figs. 27 and 28 or

$$IP = \bar{H}_{200} + \bar{T}_{850} + (-\bar{U}_{200}) + (\bar{U}_{850} - \bar{U}_{200}) + (\bar{U}_{850} - \bar{U}_{500}) \quad (2)$$

This IP parameter was designed to imply the nature of a storm's potential intensification but not necessarily the degree of that intensification. For example, if  $IP < 0$  we would expect this storm to be a non-intensifying system; if  $IP > 0$  the storm should intensify prior to landfall. There is a climatological variability in IP through the storm season and an adjustment for this variability is made to compensate for the imbalance. Discussion of the climatic variability is given in section 4.2 and details of the correction are discussed in Appendix B.

IP applied at the LF -42 time period correctly forecasts the intensity change for 71% of the 35 storms. At the LF -18 time period the skill improves to 77%. IP was plotted against the next 24 hour wind speed change for each storm and the results can be seen in Figs. 29 and 30. The statistical implications of these figures will be treated in section 5 but the two data sets appear significantly different. The exceptions of particular note in the figures are the open circles located to the left of the zero line. These data points represent the following storms: Cindy 1963, Isbell 1964, Abby 1968, Edith 1971, Carmen 1974, and Eloise 1975. A careful analysis of the weather charts for these storms revealed that they all moved into and intensified in a baroclinic region. This is precisely the kind of interaction which typically prevented the non-intensifying systems from intensifying. Perhaps these storms had different inner core characteristics and the baroclinic interaction in some way did not weaken the cyclone as is normally the case. It's possible that a measurement of the imposing

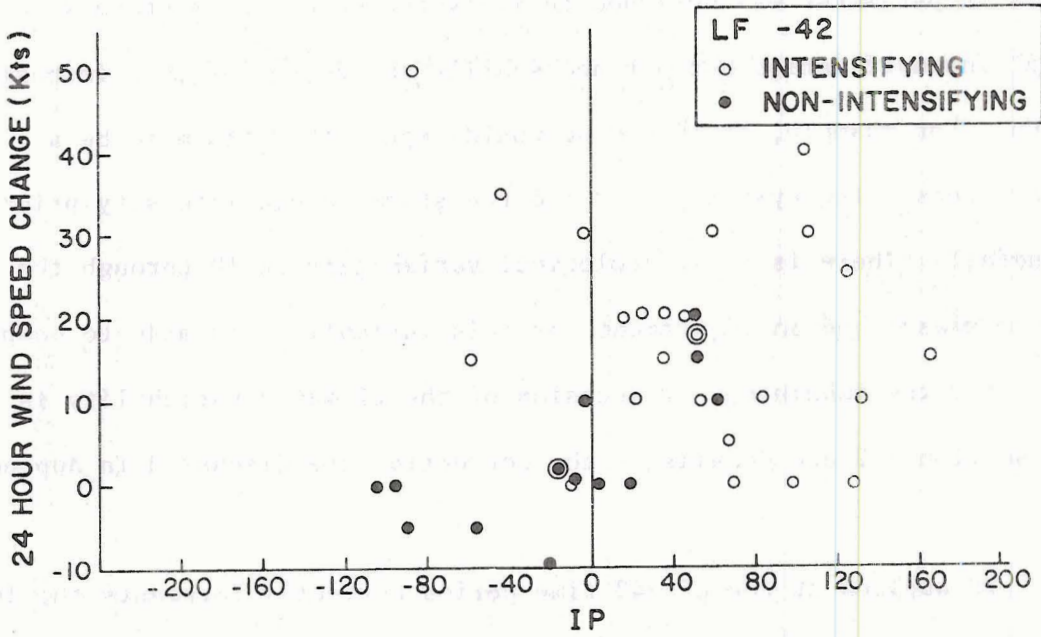


Fig. 29. Intensity change parameter (IP) vs. the next 24 hour sustained wind speed change for the LF -42 time period. Circled data points are the central values of the respective set.

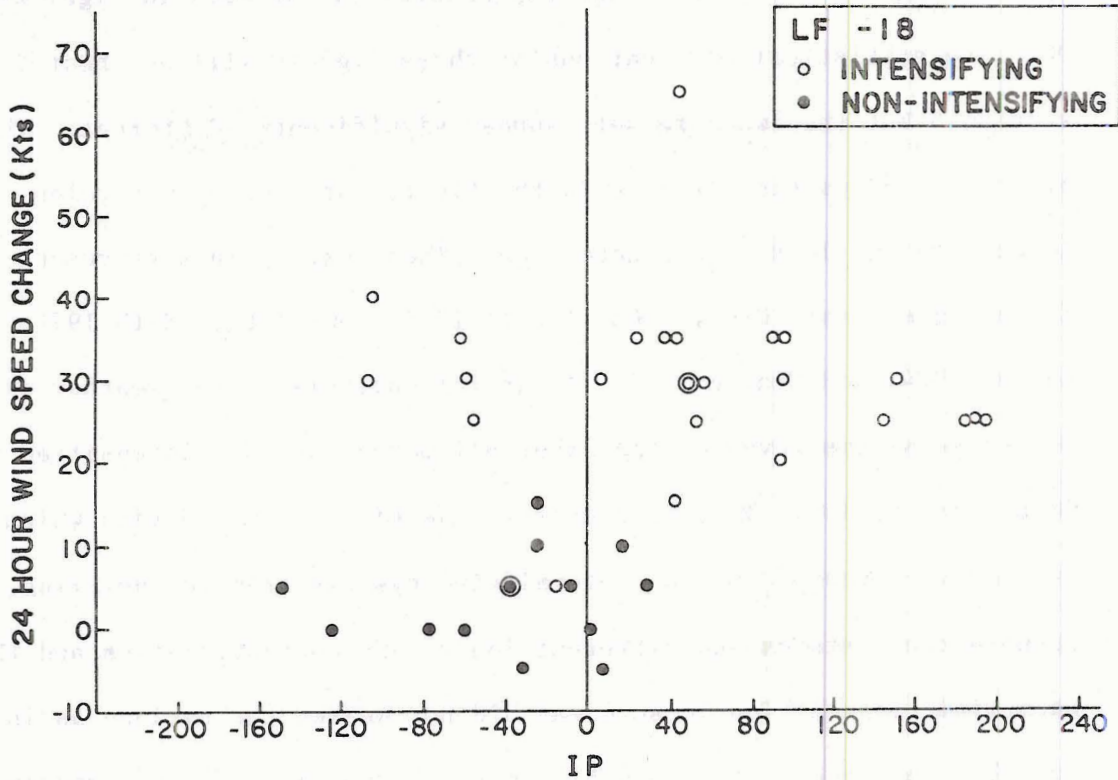


Fig. 30. Same as Fig. 29 but for the LF -18 time period.

baroclinic field alone is not enough and that there is a combination of several forces which governs intensity change. Careful budget studies (particularly angular momentum) may yield a better answer to each storm's intensification trends.

There has been confusion in regard to the interpretation of the influence of upper level troughs and baroclinicity on the poleward side of tropical cyclones. One must clearly distinguish between the typical deep layer baroclinic trough associated with middle latitude storms and the distinctly tropical upper tropospheric troughs (the so-called TUTT) often associated with tropical cyclone development within the trade winds. The TUTT is a summer phenomenon of the sub-tropical oceans and is generally favorable to the development and/or enhancement of tropical storm systems when the trough is located to the northwest of the incipient system. By contrast, a deep layer baroclinic trough is not favorable for cyclone development or enhancement. It is very important to make this distinction. This paper presents evidence on the weakening influence to cyclone strength of a deep layer baroclinic region to the cyclone's poleward side. Note in Fig. 11 that the 950-400 mb layer vertical wind shear fields between the intensifying and non-intensifying systems are very different. It is this lower and middle level baroclinicity which is the primary factor in determining cyclone weakening not upper tropospheric baroclinicity. It is very important that this distinction be appreciated.

#### 3.4 Rate of Change of IP

Another important feature of the intensity change parameter is its rate of change. Preliminary results of case studies show that when the intensity parameter registers a large increase with time, the storm

typically responds with a strong intensification within 6 to 12 hours. Conversely, a sharp decrease in IP is usually followed by a steady state or filling storm. Therefore, the initial value of IP should not be the sole determinant in forecasting storm intensity but the trend of the IP parameter should also be taken into consideration.

#### 4. APPLICATION OF IP TO INDEPENDENT DATA

It would be unfair to make general conclusions about the reliability of the intensification parameter (IP) based on only 35 cases. Therefore, the author sought independent data on which to further test the parameter. Seven cyclones from the storm seasons of 1978 and 1979 were examined. Secondly, all tropical depressions for the period 1967-1979 (23 cases) were studied. Then, the climatological and diurnal variabilities on the parameters were examined to determine the adjustments to be made to IP to allow for these variabilities. Finally, the scheme was applied to 23 independent intensity change composite data sets of the west Atlantic and west Pacific available at CSU. A listing of all additional cyclones and the analysis of the five components which go into the IP parameter are given in Tables 11-14 of Appendix A.

##### 4.1 Results of Independent Storm Analysis

Publication of west Atlantic tropical depression positions was begun in 1967 but it wasn't until 1974 that they were assigned depression numbers. Intensity changes for depressions are not included in the summaries until they reach a minimum tropical storm strength. Hence, the author had to make a general assumption that all depressions were non-intensifying systems. This is not necessarily a good assumption since depressions have been known to form in weak wave-trough systems, intensify to  $15 \text{ m s}^{-1}$  within 24 hours and then make landfall a short time later -- all criteria which would classify the system as intensifying. But for the purposes of this study all depressions will be treated equally with the exception of Depression #9 of 1975. This depression, as noted by

N. Frank (1976), was one which formed quickly and caused millions of dollars of damage in flooding as it moved inland. Although exact wind speed change was not available for this depression, indications were that it was an intensifying system.

The parameters were analyzed for all independent cyclones using the individual weather charts following the computational procedures for intensity change as discussed in Appendix B. The results of this analysis are presented in Figs. 31 and 32. Since data on the next 24 hour wind speed change was unknown for the depressions, it was assumed that these wind speed changes were zero. Even with the assumption that all depressions are non-intensifying systems we could have forecast the correct intensification trend for 15 of 20 cyclones (75%) at the LF -42 time period and 24 of 31 cyclones (77%) at the LF -18 time period. These results are comparable to those obtained from the original data sets. The big difference in examining the independent cyclone data is that the false alarm rate has increased (more cyclones forecast to intensify than actually did) but the rate of missing an intensity increase has been lowered.

Tables 7-14 of Appendix A list the data for each cyclone case. To give a better understanding of the variability of the IP parameter for each data set as listed in the tables, Fig. 33 was constructed to show how the data is distributed about the median value. The solid line represents the range over which approximately 50% of all cases fall. The dashed line gives the range in which about 70% of all cases fall. Because of the small sample size (5 cases) of the independent intensifying data set at the LF -42 time period, the solid line for this data set represents a 60% range. This figure shows no overlap between

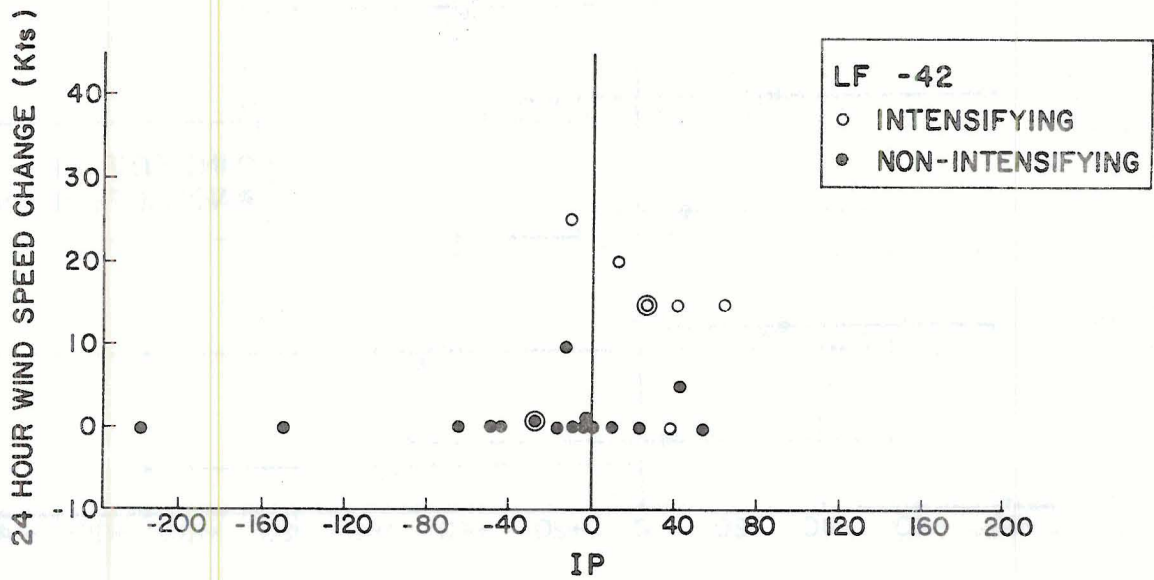


Fig. 31. Intensity change parameter (IP) versus the next 24 hour sustained wind speed change for all independent storms at the LF -42 time period. Circled data points are the central values of the respective data sets.

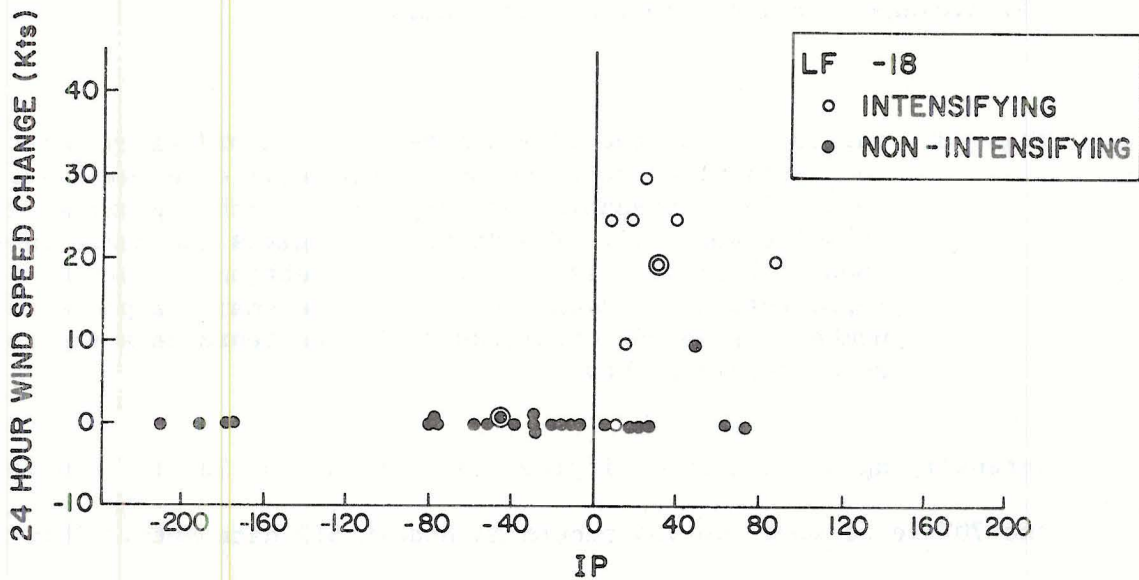
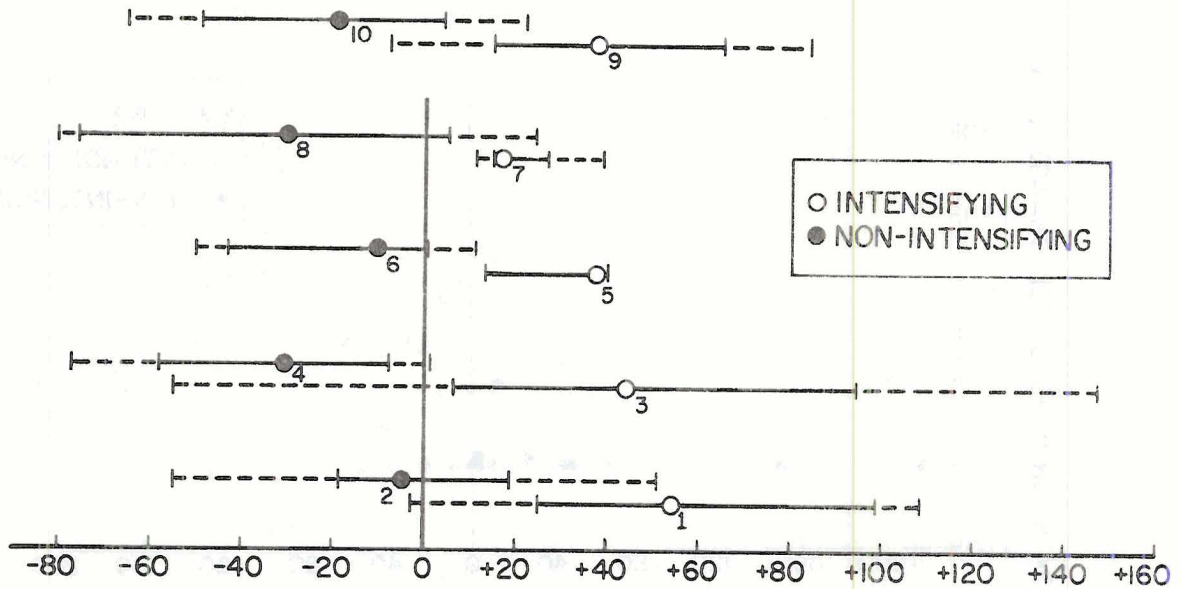


Fig. 32. Same as Fig. 31 but for the LF -18 time period.



<u>DATA SET</u>	<u>SAMPLE SIZE</u>
1. Intensifying LF -42	23
2. Non-intensifying LF -42	12
3. Intensifying LF -18	23
4. Non-intensifying LF -18	12
5. Independent intensifying LF -42	5
6. Independent non-intensifying LF -42	15
7. Independent intensifying LF -18	7
8. Independent non-intensifying LF -18	24
9. Average of all intensifying cases	58
10. Average of all non-intensifying cases	63

Fig. 33. Variability of the IP parameter for individual cyclone cases as distributed about the median value of each data set. The solid line represents the range over which approximately 50% of all cases fall. The dashed line gives the range in which about 70% of all cases fall. An exception is data set 5 which represents a 60% range because of the small sample size. The number beside the open/closed circles represents the data sets described above.

intensifying and non-intensifying cases at the 50% level. However, at the 70% level some overlap occurs in nearly all data sets. This is the indeterminant region in which the forecast errors are to be expected.

#### 4.2 Climatological and Diurnal Variation of the Parameters

The monthly distribution of intensifying vs. non-intensifying cases (Table 2 - page 15) gives indications that the differences found in the composite study may be due to climatological differences found by comparing early and late storms to those which occur during the peak of the storm season. However, after the addition of the independent cyclone data almost no such seasonal variability exists. Table 3 shows nearly an equal distribution of cyclones by month for both the intensifying and non-intensifying cyclone systems.

Seasonal climatological variations do occur in all parameters. Therefore, the IP parameter must also have a seasonal variation which must be compensated for in the forecast scheme. A ten year (1958-1967) monthly mean over 18 rawinsonde stations located in the Gulf coastal area was computed for  $\bar{H}_{200}$  and  $\bar{T}_{850}$ . The seasonal variation of these parameters is shown in Figs. 34 and 35. The dashed line in the figure is the threshold value established for the forecast scheme. Monthly mean values of the wind parameters ( $\bar{U}_{850}$ ,  $\bar{U}_{500}$  and  $\bar{U}_{200}$ ) were evaluated by averaging 5 Gulf coastal rawinsonde stations over a 5 year period (1960-1964). From these climatological measurements a monthly mean value of the IP parameter was calculated. The variations of the IP parameter are shown by the heavy solid line in Fig. 36. All cyclone cases from this study were subdivided into 15 day (half-month) periods and average IP values were computed for all cases as shown in Fig. 35. The seasonal variations of all individual cases closely parallels the climatological curve. A compensation curve to allow for these seasonal variations in the IP parameter is shown in Fig. 37. Basically, the calculated value of the IP is increased during the early and late

TABLE 3

Monthly occurrence of all cyclones which make up the study. The table includes both the individual cyclones from the composite study and the cyclones from the independent sample.

	MAY	JUN	JUL	AUG	SEP	OCT	TOTAL
INTENSIFYING	0	4	4	6	14	2	30
NON-INTENSIFYING	2	5	5	6	12	6	36

portion of the storm season and decreased during the peak of the season. Exact details of the corrections are given in Appendix B.

Diurnal variations in  $\bar{T}_{850}$  were noted when making the computations for the independent cyclone systems. The variations were particularly significant for cyclones centered in the western Gulf of Mexico where the 5-11° belt of octant 2 is located over central and west Texas. This part of Texas is slightly elevated and experiences strong surface heating. The surface heating is reflected at 850 mb where temperatures as high as 27°C were observed at 00Z in contrast to an average temperature of 17°C at 12Z. For storms in this area, only the 12Z temperature should be used. Large diurnal variations in temperature were not observed in other areas.

Diurnal variations in  $\bar{H}_{200}$  were not observed.

#### 4.3 Comparative Composite Analysis

Accepting the hypothesis that poleward baroclinic interaction causes storm weakening, it is to be expected that trends similar to those shown for the Gulf of Mexico should also occur in other ocean

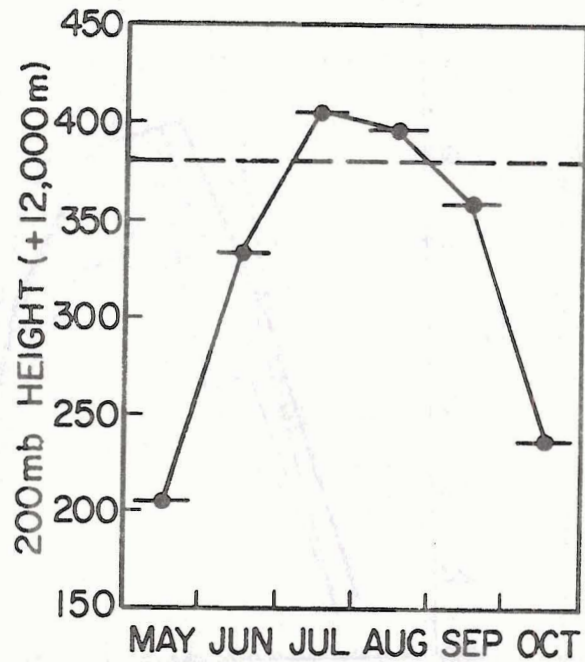


Fig. 34. Ten year (1958-1967) monthly mean of the 200 mb height averaged over 18 rawinsonde stations through the Gulf coastal area. The dashed line is the threshold value established for this study.

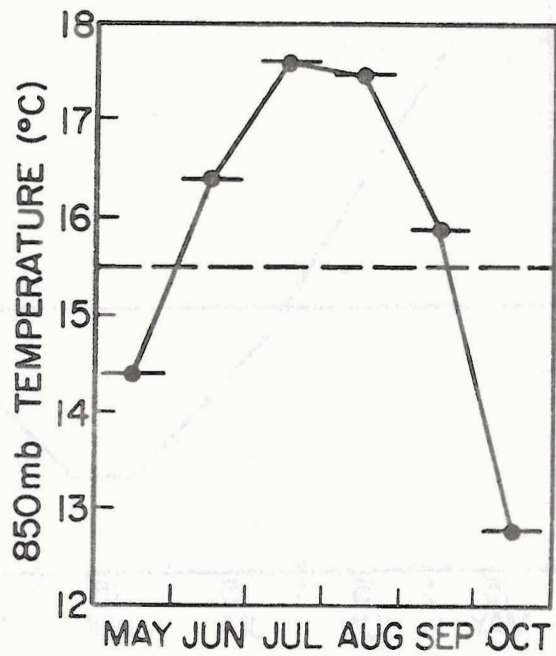


Fig. 35. Same as Fig. 34 but for the 850 mb temperature.

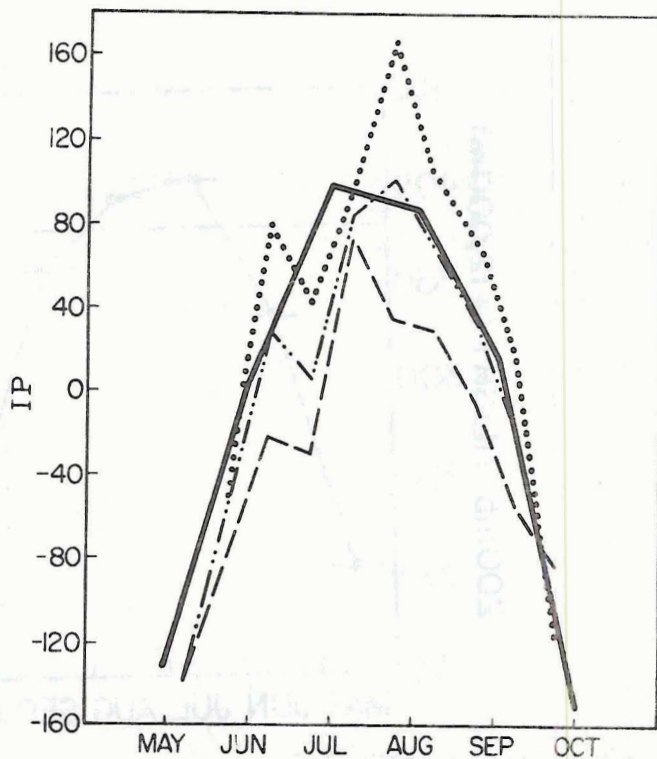


Fig. 36. Mean monthly values of IP as computed from climatology (heavy solid curve), all individual intensifying cases (dotted curve), all individual non-intensifying cases (dashed curve) and an average of both intensifying and non-intensifying cases (dash-dotted curve)

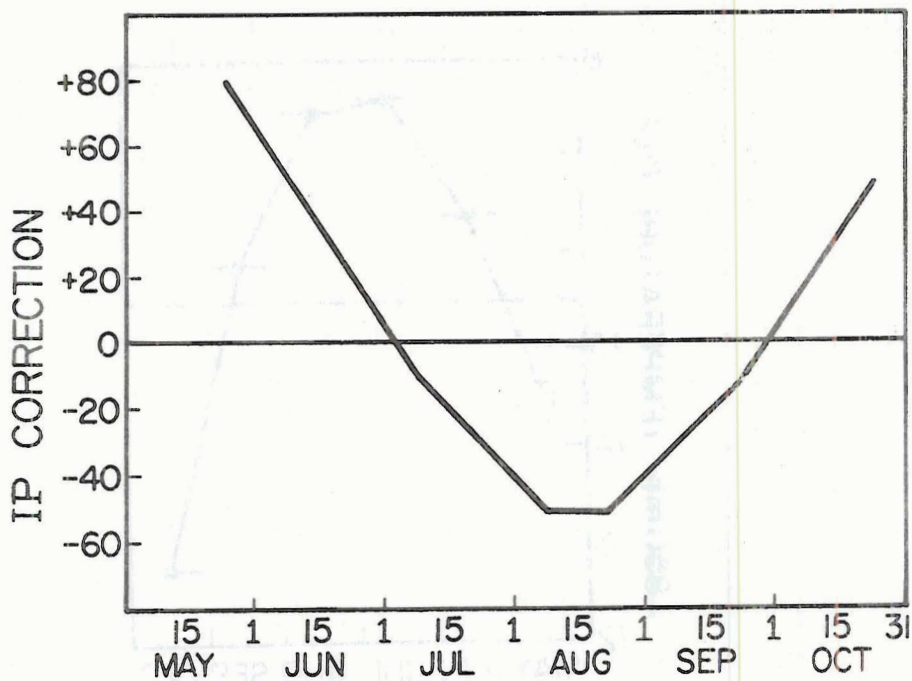


Fig. 37. Seasonal correction curve to be applied in the computation of IP.

basins. The author examined the comparative composite cyclone intensity change studies made by previous investigators at CSU -- Frank (1977), Zehr (1976) and Núñez (1981). Only those studies which contained a number of storms poleward of  $15^{\circ}$  latitude were considered. Climatologically, baroclinic troughs rarely penetrate equatorward of  $15^{\circ}$  latitude during the storm season. See Appendix C for a detailed description of each composite data set.

Analysis of these comparative composite studies (Table 4) yields results similar to those found in the Gulf of Mexico. In all filling composite data sets the intensity change parameter is significantly smaller than for the corresponding deepening set. This difference can easily be attributed to baroclinic interaction by examining the individual parameters of this table. For example, for the non-intensifying cases the westerlies are much stronger and are closer to the storm center; the vertical wind shears are much stronger; the low level temperature fields are colder; and the upper level height fields are lower.

Minor modifications had to be made to the procedures for computing IP in the Pacific basin. Climatologically, the 850 mb temperature field is warmer and the 200 mb height field is higher in the Pacific than the Atlantic. Therefore, new threshold values had to be established for these parameters. IP was computed for all data sets and the results can be seen in Fig. 38. It is most important to compare the distance separating each of the data sets rather than the relative placement on the graph. Further study in the Pacific basin needs to be done on individual cases to better refine the threshold values but the preliminary results of Fig. 38 show promise for implementation of a quantitative system for that ocean basin also. However, the climatological and diurnal effects must be examined more carefully for the Pacific basin.

TABLE 4

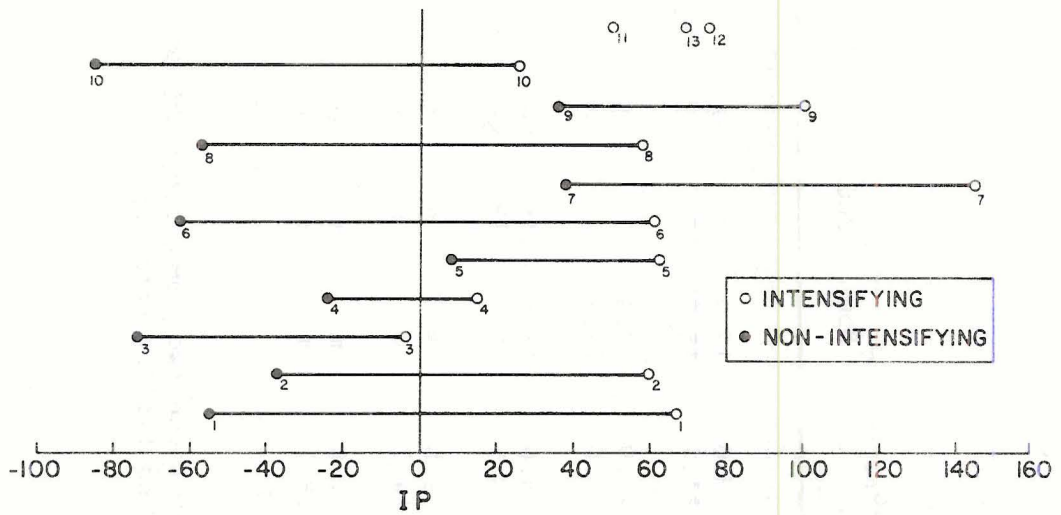
Summary of the parameters analyzed for the comparative composite studies done at CSU.  
All wind parameters are in meters,  $T_{850}$  is  $^{\circ}\text{C}$  and  $H_{200}$  is +12000 m.

COMPOSITE TITLE	$\bar{U}_{200}$	$\bar{U}_{500}$	$\bar{U}_{850}$	$\bar{U}_{850} - \bar{U}_{500}$	$\bar{U}_{850} - \bar{U}_{200}$	$\frac{6^{\circ}\text{BELT}}{\bar{U}_{200}}$	$\bar{T}_{850}$	$\bar{H}_{200}$	IP	$\Delta\text{IP}$
Dropco inten LF -42	6.7	-1.5	-4.1	-2.6	-10.8	3.4	17.4	411	68	
Dropco non-inten LF -42	17.9	1.1	-5.4	-6.5	-23.3	15.0	15.5	355	-55	123
Dropco inten LF -18	9.4	-0.2	-3.0	-2.8	-12.4	5.0	17.7	408	60	
Dropco non-inten LF -18	16.4	2.5	-2.9	-5.4	-19.3	14.9	15.9	343	-37	97
WI deep (all latitudes)	12.2	0.6	-4.4	-5.0	-16.6	10.5	16.1	374	-3	
WI fill (all latitudes)	19.1	3.7	-3.7	-7.4	-22.9	14.8	14.2	331	-74	71
WI deep ( $< 30^{\circ}$ latitude)	10.8	-0.9	-5.4	-4.5	-16.2	9.3	16.4	391	15	
WI fill ( $< 30^{\circ}$ latitude)	15.5	1.2	-5.1	-6.3	20.6	14.2	15.9	381	-24	39
Zehr develop trade clusters	2.9	-4.0	-6.9	-2.9	-9.8	1.2	17.9	468	63	
Zehr stage 0 non-develop	1.7	-3.4	-6.2	-2.8	-7.9	0.5	16.9	418	8	55
Holliday rapidly deep -24	2.1	-2.7	-5.2	-2.5	-7.3	3.6	18.5	448	50	
Holliday rapidly deep 0	4.5	-1.2	-3.8	-2.6	-8.3	0.7	18.3	472	75	
Holliday rapidly deep +24	6.7	-2.6	-5.4	-2.8	-12.1	5.4	18.4	470	69	
<u>Bill Frank Data Sets</u>										
Type A deep ( $> 20^{\circ}$ lat)	5.0	0.4	-4.1	-4.5	-9.1	2.6	18.0	473	61	
Type A fill ( $> 20^{\circ}$ lat)	16.1	4.5	-4.8	-9.3	-20.9	11.9	16.0	433	-63	124
Type A early deep ( $> 20^{\circ}$ lat)	-3.2	-1.1	-1.3	-0.2	1.9	-2.7	18.8	496	145	
Type B fill ( $> 20^{\circ}$ lat)	8.0	1.9	-3.3	-5.2	-11.3	5.7	17.9	464	38	107

TABLE 4 (cont'd)

COMPOSITE TITLE	$\bar{U}_{200}$	$\bar{U}_{500}$	$\bar{U}_{850}$	$\bar{U}_{850} - \bar{U}_{500}$	$\bar{U}_{850} - \bar{U}_{200}$	$\frac{6^\circ \text{BELT}}{\bar{U}_{200}}$	$\bar{T}_{850}$	$\bar{H}_{200}$	IP	$\Delta \text{IP}$
<u>Bill Frank data sets (cont'd)</u>										
Type A deep ( $< 30^\circ$ lat)	4.8	-1.3	-5.8	-4.5	-10.6	3.0	17.9	475	58	
Type A fill ( $< 30^\circ$ lat)	14.8	3.7	-5.3	-9.0	-20.1	11.4	15.8	436	-57	115
Type A early deep ( $< 30^\circ$ lat)	-1.5	-3.8	-5.5	-1.2	-4.0	-0.9	18.5	477	101	
Type B fill ( $< 30^\circ$ lat)	7.8	1.7	-3.6	-5.3	-11.4	5.0	17.8	461	36	65
Type I deep	5.5	-1.4	-6.2	-4.8	-11.7	4.6	18.1	448	26	
Type I fill	15.6	4.9	-4.5	-9.4	-20.1	13.5	15.3	419	-85	111
Type II deep	3.4	-0.2	-3.4	-3.2	-6.8	2.8	m <sup>1</sup>	m	m	
Type II fill	17.1	6.3	-1.8	-8.1	-18.9	14.7	m	m	m	
Type III deep	6.8	1.5	1.1	-0.4	-5.7	-1.8	m	m	m	
Type III fill	20.7	8.5	-0.1	-8.6	-29.3	18.7	m	m	m	

<sup>1</sup>These values are missing because thermodynamic runs were not made for these two composite studies. However, the wind parameters show a great disparity between the deepening and filling data sets.



Open Circles

Solid Circles

- |                                                           |    |                                                |
|-----------------------------------------------------------|----|------------------------------------------------|
| 1. Dropco Intensifying LF -42                             | vs | Dropco Non-intensifying LF -42                 |
| 2. Dropco Intensifying LF -18                             | vs | Dropco Non-intensifying LF -18                 |
| 3. West Indies Deepening (all latitudes)                  | vs | West Indies Filling (all latitudes)            |
| 4. West Indies Deepening ( $<30^{\circ}$ latitude)        | vs | West Indies Filling ( $<30^{\circ}$ latitude)  |
| 5. Zehr Developing Trade Clusters                         | vs | Zehr Stage 0 Non-developing                    |
| 6. Frank Type A Deepening ( $>20^{\circ}$ latitude)       | vs | Frank Type A Filling ( $>20^{\circ}$ latitude) |
| 7. Frank Type A Early Deepening ( $>20^{\circ}$ latitude) | vs | Frank Type B Filling ( $>20^{\circ}$ latitude) |
| 8. Frank Type A Deepening ( $<30^{\circ}$ latitude)       | vs | Frank Type A Filling ( $<30^{\circ}$ latitude) |
| 9. Frank Type A Early Deepening ( $<30^{\circ}$ latitude) | vs | Frank Type B Filling ( $<30^{\circ}$ latitude) |
| 10. Frank Type I Deepening                                | vs | Frank Type I Filling                           |
| 11. Holliday Rapidly Deepening -24                        |    |                                                |
| 12. Holliday Rapidly Deepening 0                          |    |                                                |
| 13. Holliday Rapidly Deepening +24                        |    |                                                |

Fig. 38. Graph of IP for comparative intensity change rawinsonde composite data sets. Numbers denote each composite data set comparison. The line between the data points shows the difference between the intensifying and non-intensifying data sets. See Appendix C for a detailed description of all data sets.

This forecasting scheme was also applied to a set of rapidly deepening typhoons (deepening rate  $\geq 42 \text{ mb d}^{-1}$ ) from the northwest Pacific which was studied by Holliday and Thompson (1979). IP was determined from rawinsonde composites prepared for these storms for three time periods (RD-24, RD-0, RD+24) as described in Appendix C. Computations of IP made for these Holliday and Thompson cases indicated that intensification should occur. Close analysis of the parameters which determine IP (Table 4) revealed that a large part of the increase in IP between time periods for this data set was due to changes in the 200 mb height field. It appeared that the storms were moving into an area of higher 200 mb heights ( $> 12470 \text{ m}$ ) as the rapid deepening was occurring. Indications are that it may be just as important to watch for changes in the individual parameters as well as the total change in IP.

Discussion. This section has provided more verification that baroclinic interaction does in fact modify a storm's intensity and more importantly that the interaction can be measured in a quantitative sense. The skill of making forecasts using this quantitative scheme has been shown to be  $> 70\%$  correct. The author is hopeful that through further refinements this forecast skill can be increased somewhat.

## 5. STATISTICAL ANALYSIS

The data as presented in this study appear to be highly significant. To determine the level of significance of these results, all data were examined collectively for the time periods LF -42 and LF -18. The statistical methods used for these non-parametric data sets were contingency tables, prefigurance - post agreement, skill scores and the recently developed technique termed Multi-Response Permutation Procedures (MRPP). A complete description of the MRPP technique can be found in Mielke et al. (1976, 1981) and Mielke (1979).

### 5.1 Contingency Tables

Contingency tables represent a means of testing the discrepancy between observed results and those expected under the proposed forecasting parameter. Two by two contingency tables were used to plot future forecast intensification (I) and non-intensification (NI) against that actually observed (Fig. 39). For this statistical test any cyclone which experienced a wind speed change  $\geq 10$  kts over the next 24 hour period was considered an intensifying system. Figure 40 shows the no-skill table that would have resulted if the forecaster really had no skill and his correct forecasts were due to random probability. This no-skill table is formed from Fig. 39 by multiplying row totals by column totals and then dividing by the grand total. Using these two tables we can then compute the chi-square statistic by

$$\chi^2 = \sum_{i=1}^4 \frac{(O_i - H_i)^2}{H_i}$$

LF -42 OBSERVED				LF -18 OBSERVED				
FORECAST		I	NI	TOTAL		I	NI	TOTAL
	I	20	11	31	I	25	9	34
	NI	5	19	24	NI	6	26	32
	TOTAL	25	30	55	TOTAL	31	35	66

Fig. 39. Contingency tables made from all storm cases for the LF - 42 time period (left diagram) and the LF -18 time period (right diagram).

LF -42 OBSERVED				LF -18 OBSERVED				
FORECAST		I	NI	TOTAL		I	NI	TOTAL
	I	14	17	31	I	16	18	34
	NI	11	13	24	NI	15	17	32
	TOTAL	25	30	55	TOTAL	31	35	66

Fig. 40. No-skill table made from the contingency tables in Fig. 39 by multiplying the row total by the column total and dividing by the grand total. Left diagram is for LF -42 time period and right diagram is for the LF -18 time period.

where  $O_i$  is the observed counts (Fig. 39) and  $H_i$  is the no-skill counts (Fig. 40). We find that for the time period LF -42,  $\chi^2 = 12.4$  and at LF -18,  $\chi^2 = 19.7$ . Using chi-square tables with one degree of freedom, we find that for both time periods the probability value for chi-square is less than 0.001 that a no-skill forecast would have led to the given verification tables (Fig. 39).

The usefulness of the predictor can also be determined by forming contingency ratios (Fig. 41). These are simply the ratios of the numbers in the contingency tables (Fig. 39) to the numbers in the corresponding no-skill tables (Fig. 40). Whenever these ratios are greater than unity, the relationship between the predictor and outcome is much better than a chance one. As we can see from Fig. 41 the forecasting parameter is significantly better than chance in forecasting both intensification and non-intensification.

## 5.2 Prefigurance - Post Agreement

Prefigurance measures the extent to which forecasts give advance notice of the occurrence of a certain event. Post agreement gives the

		LF -42 OBSERVED		LF -18 OBSERVED	
		I	NI	I	NI
F O R E C A S T	I	1.43	.65	1.56	.50
	NI	.45	1.46	.40	1.53

Fig. 41. Contingency ratios formed by dividing the values in the contingency tables (Fig. 39) by the values in the no-skill tables (Fig. 40). Left diagram is for LF -42 time period and right diagram is for LF -18 time period.

extent to which subsequent observations confirm the predictions when a certain event is forecast. This information can be found by using the previously constructed contingency tables (Fig. 39) to develop the tables found in Figs. 42 and 43. The data from these figures is condensed below:

TABLE 5

	Prefigurance (Percentage Accuracy)		Post Agreement (Percentage Accuracy)	
	<u>I</u>	<u>NI</u>	<u>I</u>	<u>NI</u>
LF -42	80	63	65	79
LF -18	81	74	74	81

As an example of the use of Table 5, we might consider the LF -42 time period. We see that forecasts of intensification were followed by intensification 65% of the time while occurrences of intensification were indicated in advance 80% of the time. The trend in the scheme is to over forecast intensification while under forecasting non-intensification.

### 5.3 Skill Scores

The information contained in the contingency tables can be combined into a single index (S), called a skill score. It is defined by

$$S = \frac{C - E}{T - E}$$

where C is the number of correct forecasts, T is the total number of forecasts and E is the number expected to be correct by chance. Skill scores were computed for the two time periods and found to be .43 and .55 for the LF -42 and LF -18 time periods respectively. These numbers

		LF -42 OBSERVED		LF -18 OBSERVED	
FORECAST		I	NI	I	NI
I	80	37	81	26	
NI	20	63	19	74	
TOTAL	100	100	100	100	

Fig. 42. Percent of time each observed category was correctly forecast (Prefigurance).

		LF -42 OBSERVED			LF -18 OBSERVED		
FORECAST		I	NI	TOTAL	I	NI	TOTAL
I	65	35	100	74	26	100	
NI	21	79	100	19	81	100	

Fig. 43. Percent of time each forecast event occurred for a particular category (Post Agreement).

represent an average correct forecast rate of 75% which beats chance by 25%.

#### 5.4 MRPP

The MRPP technique which has been developed at CSU (cf. Mielke et. al., 1976, 1981; Mielke, 1979) is a nonparametric statistical methodology which does not involve normality or other assumptions usually made in statistical analyses. It allows the simultaneous comparison of one or more variates of one data set with the same variates of other data sets. The procedure essentially measures the Euclidean distance between all data points giving the likelihood of one set of data being statistically the same as an opposing data set. The MRPP technique was applied to the data of this study in three ways:

- 1) All parameters were examined univariately comparing the intensifying versus non-intensifying set.
- 2) The three most significant parameters,  $\bar{H}_{200}$ ,  $\bar{T}_{850}$  and  $\bar{U}_{200}$  ( $6^{\circ}$  belt) were combined in a three-way combination.
- 3) All five parameters were examined in a five-way combination.

The results of the analysis are shown in Table 6. One can see that the vertical wind shears are the weakest parameters but when combined with the other parameters to form IP, the results become extremely significant.

The MRPP statistic can also be used to improve the selection of parameters in devising a forecasting scheme. For example, in the NW Pacific, data is less abundant particularly at the 500 mb level. Therefore, use of the scheme without the contribution of the 850 to 500 mb shear should also give good results. In fact the MRPP results indicate that the 200 mb height field alone may be sufficient to produce a reasonable forecast.

TABLE 6

MRPP significance levels on probability that the intensifying and non-intensifying data sets are the same. Parameters are listed in order of significance as determined by an average of both time periods. Values are given in percent (%).

PARAMETER	SIGNIFICANCE LEVEL	
	LF -42	LF -18
IP	.00772	.000878
5 Way Combination <sup>1</sup>	.0576	.000288
3 Way Combination <sup>2</sup>	.0752	.000275
$\bar{H}_{200}$	.0787	.000288
$\bar{T}_{850}$	.323	.0035
$\bar{U}_{200}$ (6° belt)	1.18	.0724
$\bar{U}_{850} - \bar{U}_{200}$	.140	1.31
$\bar{U}_{850} - \bar{U}_{500}$	.230	3.56

<sup>1</sup> 5 Way combination consists of all five parameters.

<sup>2</sup> 3 Way combination consists of  $\bar{H}_{200}$ ,  $\bar{T}_{850}$  and  $\bar{U}_{200}$  (6° belt).

Discussion. The four statistical methods had all shown that the results produced by the forecasting scheme are highly significant. This allows us to adapt the scheme to operational usage with a high degree of confidence. However, we must remember that this scheme is an objective tool designed to be used by less experienced forecasters and may only be of minor help for the experienced forecaster.

## 6. CONCLUSION

The original goals of this research were to detect systematic outer cyclone (3-12<sup>0</sup> radius) meteorological differences between intensifying and non-intensifying storms merely by examining the tropical weather charts available at the National Hurricane Center. But many hours of tedious study of these charts could only give weak subjective indications of possible baroclinic influences on cyclone intensity change. Therefore, the rawinsonde compositing scheme was employed in order to investigate quantitative differences in an objective manner. Composite differences were found to be significant. Of particular interest were the differences found in the 850 mb temperature field, the 200 mb height field, the 200 mb zonal wind, and vertical wind shears of the zonal wind.

Based on the results obtained from the composite study the individual cyclones were again analyzed for these special parameter differences. Some variability was inherent in the results, but a distinct demarcation between the two data sets was evident in 70-80% of the cases. Special combinations of the parameters led to a quantitative scheme for forecasting tropical cyclone intensity change.

This forecast scheme held up well when tested against independent data. The scheme was able to forecast intensity change 71-77% correct for all time periods and was at its best as the cyclones were within 24 hours of landfall. It was found that trends in the parameters should also be carefully watched as indicators of intensity change. Through the use of previous comparative rawinsonde composite studies, we were able to show that the results of this study are applicable to composite data sets (and mostly likely individual cases also) in the other regions of the west Atlantic and also in the western Pacific.

The forecasting scheme presented in this study may not significantly exceed the accuracy of the forecasts produced by the experts at the National Hurricane Center or the Joint Typhoon Warning Center but it does give quantitative guidance to the parameters which appear to be important to intensity change. Because the scheme was designed for use on standard isobaric charts, any duty forecaster (regardless of experience) should be able to make the IP computation within 10-15 minutes. Also, the selection of the 850 and 200 mb charts allows one to supplement the standard analysis at these levels with SMS satellite derived winds. The scheme can also be programmed for routine computer printout.

Although this study failed to correctly predict intensity change in approximately 25% of the cases, the scheme appears to perform as well or better than other currently available forecasting techniques. You will always have an Eloise to defy your best physical reasoning. However, the idea that intensity change can be approached in a quantitative manner bears further investigation. More research should be made to determine how the physical coupling between tropical storms and the large scale baroclinic zones on the poleward side takes place. Hopefully, some of the ideas presented in this study will stimulate further cyclone intensity research.

An additional side benefit of this study, in addition to the particular results presented on cyclone intensity change, is the formulation of a methodological technique for quantitative forecast development through the use of rawinsonde composite analysis. This methodology is summarized by the progressive steps of route B in Fig.44.

Quantitative forecast schemes cannot typically be developed from direct inspection of individual weather maps as indicated by route A of

Fig. 44 (i.e., going directly from step 2 to step 9). One is usually required to follow the procedures illustrated in route B of this figure. A quantitative forecast scheme development usually requires the evaluation of numerous rawinsonde reports from different classes of weather systems to determine mean differences between classes. Only when this is accomplished can one begin testing to determine the extent to which such mean class parameter differences can be detected in individual case situations. In this manner the rawinsonde compositing technique has been used as a vehicle to transport us from a general idea to a specific application. Then thorough statistical testing to determine forecast skill, testing with other independent data sets, etc., follows in logical progression as shown by route B of this figure.

The research meteorologist can only carry the procedures as far as step 8. The final testing of any new forecast scheme must be done in the operational environment by operational meteorologists (step 9).

It is anticipated that this empirical methodological approach using composite rawinsonde data can be utilized to develop many other types of practical forecast schemes.

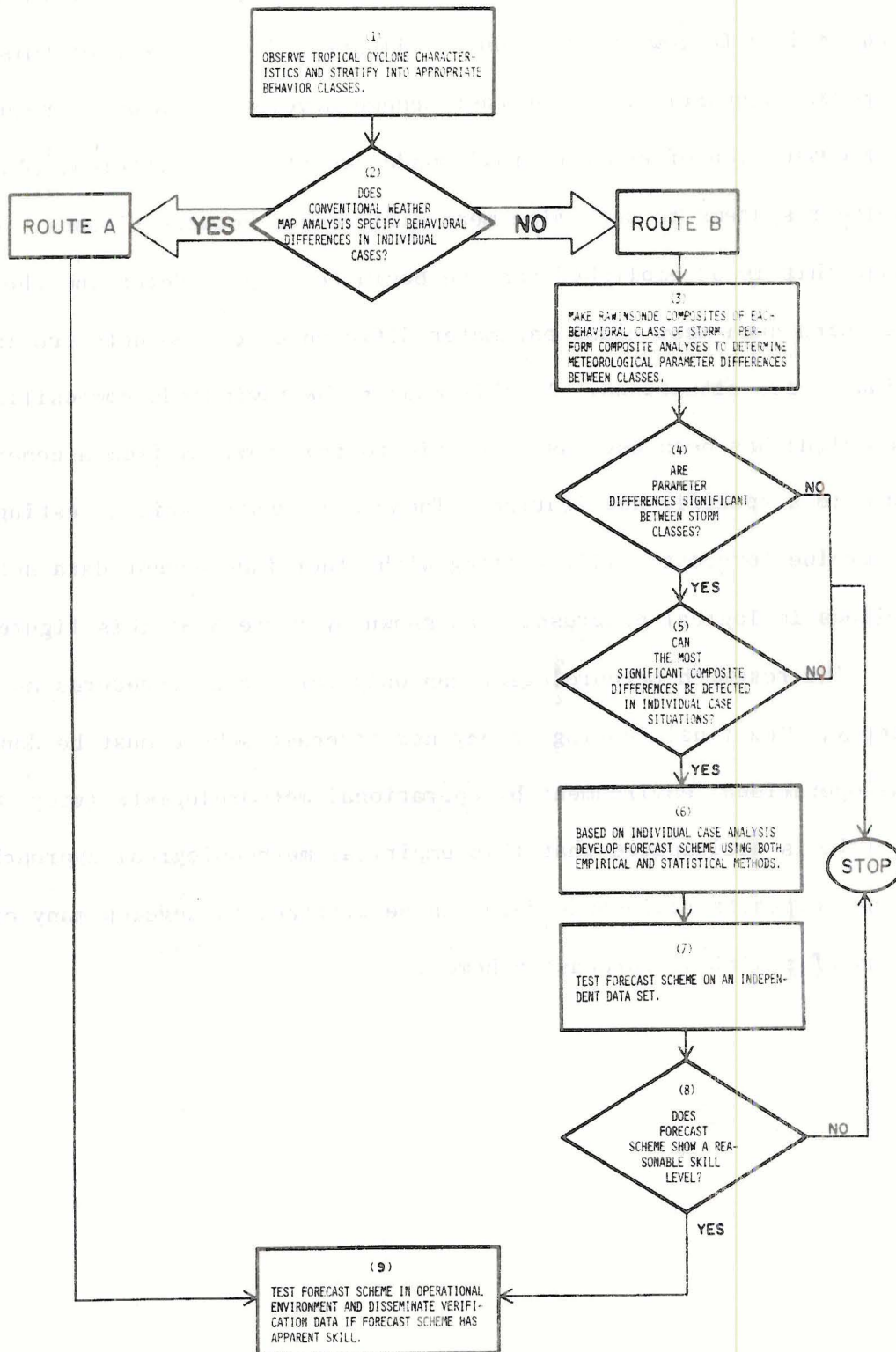


Fig. 44. Flow diagram of the procedures needed to develop an empirical forecast scheme. This study followed the procedures outlined by Route B where rawinsonde compositing (step 3) was an integral and necessary step.

## ACKNOWLEDGEMENTS

The author wishes to acknowledge the guidance and continued encouragement given him by his adviser, Professor William M. Gray. The author has been fortunate to have had the rawinsonde data base of Professor Gray's research project available to him. The author would also like to thank Mr. Edwin Buzzell and Mrs. Barbara Brumit for their technical assistance. The author has also benefited from discussions with Dr. Edwin Núñez (now of the University of Puerto Rico), Mr. Geoff Love, Mr. Greg Holland, Mr. Cheng Shang Lee, Mr. Johnny Chan and Mr. Robert Merrill of the CSU tropical cyclone research project. The author also acknowledges the US Air Force for providing the author the opportunity to attend Colorado State University.

This research has been supported by the National Oceanic and Atmospheric Administration Grant No. NA 79 RAD00002.

## REFERENCES

- Arnold, C. P., 1977: Tropical cyclone cloud and intensity relationships. Dept. of Atmos. Sci. Paper No. 277, Colo. State Univ., Ft. Collins, CO, 154 pp.
- Dunn, G. E. and Staff, 1962: The hurricane season of 1961. Mon. Wea. Rev., 90, 107-119.
- Dunn, G. E. and Staff, 1963: The hurricane season of 1962. Mon. Wea. Rev., 91, 199-207.
- Dunn, G. E. and Staff, 1964: The hurricane season of 1963. Mon. Wea. Rev., 92, 128-138.
- Dunn, G. E. and Staff, 1965: The hurricane season of 1964. Mon. Wea. Rev., 93, 175-187.
- Erickson, S. L., 1977: Comparison of developing vs. non-developing tropical disturbances. Dept. of Atmos. Sci. Paper No. 274, Colo. State Univ., Ft. Collins, CO, 81 pp.
- Frank, N. L., 1970: Atlantic tropical systems of 1969. Mon. Wea. Rev., 98, 307-314.
- Frank, N. L., 1971: Atlantic tropical systems of 1970. Mon. Wea. Rev., 99, 281-285.
- Frank, N. L., 1972: Atlantic tropical systems of 1971. Mon. Wea. Rev., 100, 268-275.
- Frank, N. L., 1973: Atlantic tropical systems of 1972. Mon. Wea. Rev., 101, 334-338.
- Frank, N. L., 1975: Atlantic tropical systems of 1974. Mon. Wea. Rev., 103, 294-300.
- Frank, N. L., 1976: Atlantic tropical systems of 1975. Mon. Wea. Rev., 104, 466-474.
- Frank, N. L. and G. Clark, 1977: Atlantic tropical systems of 1976. Mon. Wea. Rev., 105, 676-683.
- Frank, N. L. and G. Clark, 1978: Atlantic tropical systems of 1977. Mon. Wea. Rev., 106, 559-565.
- Frank, N. L. and G. Clark, 1979: Atlantic tropical systems of 1978. Mon. Wea. Rev., 107, 1035-1041.
- Frank, N. L. and G. Clark, 1980: Atlantic tropical systems of 1979. Mon. Wea. Rev., 108, 966-972.

## REFERENCES (cont'd)

- Frank, N. L. and P. J. Hebert, 1974: Atlantic tropical systems of 1973. Mon. Wea. Rev., 102, 290-295.
- Frank, W. M., 1976: The structure and energetics of the tropical cyclone. Dept. of Atmos. Sci. Paper No. 258, Colo. State Univ., Ft. Collins, CO, 180 pp.
- Gray, W. M., 1968: Global view of the origin of tropical disturbances and storms. Mon. Wea. Rev., 96, 669-700.
- Gray, W. M., 1975: Tropical cyclone genesis. Dept. of Atmos. Sci. Paper No. 234, Colo. State Univ., Ft. Collins, CO, 121 pp.
- Gray, W. M., 1980: Observational and theoretical aspects of tropical cyclone genesis. Report prepared as a result of the author's appointment as an adjunct research professor of meteorology at the US Naval Postgraduate School, Monterey, CA, from 7 July to 7 August 1980, 71 pp.
- Gray, W. M. and W. M. Frank, 1977: Tropical cyclone research by data compositing. NEPRF Technical Report TR-77-01. Naval Environmental Prediction Research Facility, Monterey, CA, 70 pp.
- Gray, W. M. and W. M. Frank, 1978: New results of tropical cyclone research from observational analysis. Technical Report TR-78-01, Naval Environmental Prediction Research Facility, Monterey, CA, 105 pp.
- Hebert, P. J., 1976: Atlantic hurricane season of 1975. Mon. Wea. Rev., 104, 453-465.
- Hebert, P. J., 1978: Intensification criteria for tropical depressions of the western north Atlantic. Mon. Wea. Rev., 106, 831-840.
- Hebert, P. J., 1980: Atlantic hurricane season of 1979. Mon. Wea. Rev., 108, 973-990.
- Hebert, P. J. and N. L. Frank, 1974: Atlantic hurricane season of 1973. Mon. Wea. Rev., 102, 280-289.
- Holliday, C. R. and A. H. Thompson, 1979: Climatological characteristics of rapidly intensifying typhoons. Mon. Wea. Rev., 107, 1022-1034.
- Hope, J. R., 1975: Atlantic hurricane season of 1974. Mon. Wea. Rev., 103, 285-293.
- Jarvinen, B. R. and C. J. Neumann, 1979: Statistical forecasts of tropical cyclone intensity for the north Atlantic basin. NOAA Tech. Memorandum NWS NHC-10 National Hurricane Center, Miami, FL, 22 pp.

## REFERENCES (cont'd)

- Lawrence, M. B., 1977: Atlantic hurricane season of 1976. Mon. Wea. Rev., 105, 497-507.
- Lawrence, M. B., 1978: Atlantic hurricane season of 1977. Mon. Wea. Rev., 106, 534-545.
- Lawrence, M. B., 1979: Atlantic hurricane season of 1978. Mon. Wea. Rev., 107, 477-491.
- McBride, J. L., 1981: Observational analysis of tropical cyclone formation, Part I: Basic description of data sets. J. Atmos. Sci.
- McBride, J. L. and R. Zehr, 1981: Observational analysis of tropical cyclone formation, Part II: Comparison of non-developing versus developing systems. J. Atmos. Sci.
- Mielke, P. W., 1979: An asymptotic non-normality of null distributions of MRPP statistics. Commun. Statist. -Theor. Meth., A8, 1541-1550.
- Mielke, P. W., K. J. Berry and E. S. Johnson, 1976: Multi-response permutation procedures for a priori classification. Commun. Statist.-Theor. Meth., A5, 1409-1424.
- Mielke, P. W., Jr., K. J. Berry and G. W. Brier, 1981: Application of multi-response permutation procedure for examining seasonal changes in monthly mean sea-level pressure patterns. Mon. Wea. Rev., 109, 120-126.
- Mosteller, F. and R. E. K. Rourke, 1973: Sturdy statistics. Reading, MA, Madison-Wesley, 394 pp.
- Neumann, C. J., G. W. Cry, E. L. Caso and B. R. Jarvinen, 1978: Tropical cyclones of the North Atlantic Ocean, 1871-1977. Asheville, NC, U.S. Government Printing Office, 1978, 170 pp.
- Núñez, E., 1981: Tropical cyclone structure and intensity change. Dept. of Atmos. Sci. Ph. D. Thesis, Colo. State Univ., Ft. Collins, CO, 192 pp.
- Panofsky, H. A. and G. W. Brier, 1968: Some applications of statistics to meteorology. University Park, PA: The Pennsylvania State Univ., 224 pp.
- Ramage, C. S., 1974: The typhoons of October 1970 in the south China Sea: Intensification, decay and ocean interaction. J. Appl. Meteor., 13, 739-751.
- Ruprecht, E. and W. M. Gray, 1976: Analysis of satellite-observed tropical cloud clusters, Part I: Wind and dynamic fields. Tellus, 28, 391-413.

## REFERENCES (cont'd)

- Simpson, R. H. and P. J. Hebert, 1973: Atlantic hurricane season of 1972. Mon. Wea. Rev., 101, 323-333.
- Simpson, R. H. and J. R. Hope, 1972: Atlantic hurricane season of 1971. Mon. Wea. Rev., 100, 256-267.
- Simpson, R. H. and J. M. Pelissier, 1971: Atlantic hurricane season of 1970. Mon. Wea. Rev., 99, 269-277.
- Simpson, R. H., A. L. Sugg and Staff, 1970: Atlantic hurricane season of 1969. Mon. Wea. Rev., 98, 293-306.
- Simpson, R. H., N. Frank, D. Shideler and H. M. Johnson, 1968. Atlantic tropical disturbances, 1967. Mon. Wea. Rev., 96, 251-259.
- Simpson, R. H., N. Frank, D. Shideler and H. M. Johnson, 1969: Atlantic tropical disturbances of 1968. Mon. Wea. Rev., 97, 240-255.
- Sugg, A. L., 1966: The hurricane season of 1965. Mon. Wea. Rev., 94, 183-191.
- Sugg, A. L., 1967: The hurricane season of 1966. Mon. Wea. Rev., 95, 131-142.
- Sugg, A. L. and P. J. Hebert, 1969: The Atlantic hurricane season of 1968. Mon. Wea. Rev., 97, 225-239.
- Sugg, A. L. and J. M. Pelissier, 1968: The hurricane season of 1967. Mon. Wea. Rev., 96, 242-250.
- Williams, K. and W. M. Gray, 1973: Statistical analysis of satellite observed cloud clusters in the western Pacific. Tellus, 21, 313-336.
- Zehr, R., 1976: Tropical disturbance intensification. Dept. of Atmos. Sci. Paper No. 259, Colc. State Univ., Ft. Collins, CO, 91 pp.

## APPENDIX A

Appendix A is a summary of the parameters analyzed for all storms which make up this study. Tables 7-10 represent the data for the original composite study. Tables 11-14 list all results for the independent storms which were tested. All parameters analyzed (except  $6^\circ$  belt  $\bar{U}_{200}$ ) represent the  $5-11^\circ$  belt average over octants 8, 1 and 2. Units for the respective parameters are as follows:

zonal wind parameters ( $\bar{U}_{850}$ , $\bar{U}_{500}$ , $\bar{U}_{200}$ )	$\text{m s}^{-1}$
vertical zonal wind shear ( $\bar{U}_{850} - \bar{U}_{500}$ , $\bar{U}_{850} - \bar{U}_{200}$ )	$\text{m s}^{-1}$
temperature field ( $\bar{T}_{850}$ )	$^\circ\text{C}$
height field ( $\bar{H}_{200}$ )	+12000 m
intensification parameter (IP)	no units
wind speed change	kts

TABLE 7

Summary of the parameters analyzed for the intensifying set at the LF -18 time period

YR	STORM NAME	$\bar{U}_{200}$	$\bar{U}_{500}$	$\bar{U}_{850}$	$\bar{U}_{850} - \bar{U}_{500}$	$\bar{U}_{850} - \bar{U}_{200}$	$\frac{6}{U_{200}} \text{BELT}$	$\bar{T}_{850}$	$\bar{H}_{200}$	IP	NEXT 24 HOUR WIND SPEED CHANGE
57	Audry	13.7	0.9	-1.4	- 2.3	- 15.1	10.5	18.4	357	42	35
57	Bertha	-16.9	-5.0	-2.4	2.6	+ 14.5	- 20.9	17.5	476	195	25
59	Debra	9.0	2.0	-0.3	- 2.3	- 9.3	8.4	19.4	423	56	30
59	Judith	18.0	5.0	-0.6	- 5.6	- 18.6	8.0	17.3	444	94	30
61	Carla	10.5	-4.6	-7.7	- 3.1	- 18.2	8.3	18.5	456	41	15
63	Cindy	17.1	2.9	-3.5	- 6.4	- 20.6	15.6	15.4	386	-60	30
64	Abby	- 3.1	-5.8	-2.2	+ 3.6	+ 0.9	- 5.3	21.1	475	153	30
64	Isbell	30.3	6.6	-6.2	-12.8	- 36.5	24.2	15.0	350	-109	30
65	Betsy	1.4	-5.5	-6.6	- 1.1	- 8.0	3.6	16.6	456	92	20
67	Beulah	15.9	-0.5	-4.7	- 4.2	- 20.6	7.8	16.7	401	6	30
68	Abby	19.1	2.9	-2.8	- 5.7	- 21.9	20.7	16.3	327	-15	5
68	Candy	8.1	0.0	-3.6	- 3.6	- 11.7	2.9	18.2	414	95	35
69	Camille	10.6	3.4	-0.8	- 4.2	- 11.4	7.4	18.3	437	23	35
70	Celia	- 5.4	-2.2	-0.6	+ 1.6	+ 4.8	- 4.5	19.9	482	147	25
70	Ella	7.7	0.5	-4.7	- 5.2	- 12.4	7.4	18.2	433	37	35
70	Felice	-14.3	-7.9	-5.8	+ 2.1	+ 8.5	- 19.9	17.4	474	193	25
71	Edith	25.4	2.0	-0.5	- 2.5	- 25.9	26.1	18.9	330	-62	35
74	Carmen	16.8	4.1	-2.5	- 6.6	- 19.3	14.7	15.9	376	-55	25
75	Caroline	- 1.1	-2.3	-1.8	+ 0.5	- 0.7	- 6.6	18.8	409	89	35
75	Eloise	20.5	6.3	-4.8	-11.1	- 25.3	12.7	14.0	319	-104	40
77	Anita	2.9	-3.3	-5.6	- 2.3	- 8.5	3.1	18.4	434	44	65
77	Babe	7.3	-0.9	-3.4	- 2.5	- 10.7	2.8	18.0	424	52	25
	Average	8.8	-0.1	-3.3	- 3.2	- 12.1	5.8	17.6	413	49	29.8

TABLE 8

Summary of the parameters analyzed for the intensifying set at the LF -42 time period

YR	STORM NAME	$\bar{U}_{200}$	$\bar{U}_{500}$	$\bar{U}_{850}$	$\bar{U}_{850} - \bar{U}_{500}$	$\bar{U}_{850} - \bar{U}_{200}$	$6^{\circ}\text{BELT}$ $\bar{U}_{200}$	$\bar{T}_{850}$	$\bar{H}_{200}$	IP	NEXT 24 HOUR WIND SPEED CHANGE
57	Audry	17.4	- 0.9	- 0.3	+ 0.6	- 17.7	17.3	16.4	391	25	20
57	Bertha	3.4	- 5.0	- 3.1	+ 1.9	- 6.5	5.7	16.6	406	22	10
59	Debra	5.6	2.1	- 1.1	- 3.2	- 6.7	1.6	19.3	434	81	10
59	Judith	3.6	- 2.7	- 4.2	- 1.5	- 7.8	1.6	18.3	439	163	15
61	Carla	8.0	- 6.9	- 8.3	- 1.4	- 16.3	3.5	17.8	427	38	20
63	Cindy	22.8	4.8	- 2.4	- 7.2	- 25.2	19.3	16.4	337	-57	15
64	Abby	8.3	- 0.6	- 4.2	- 3.6	- 12.5	8.5	20.6	483	68	0
64	Isbell	25.4	9.8	- 6.5	-16.3	- 31.9	17.6	14.9	362	-84	50
65	Betsy	- 6.8	- 8.2	-12.1	- 3.9	- 5.3	10.1	15.8	395	68	5
67	Beulah	9.6	- 1.2	- 4.1	- 2.9	- 13.7	9.0	17.3	410	35	15
68	Abby	18.8	1.5	- 6.5	- 8.0	- 25.3	11.7	16.1	335	-3	30
68	Candy	0.0	1.8	+ 1.4	- 0.4	+ 1.4	0.0	17.8	401	131	10
69	Camille	3.7	0.3	- 1.3	- 1.6	+ 5.0	5.5	17.9	417	59	30
70	Celia	- 4.5	- 0.2	0.3	+ 0.5	+ 4.8	2.6	19.1	465	124	25
70	Ella	- 6.0	- 5.4	- 4.3	+ 1.1	+ 1.7	2.1	17.5	436	105	40
70	Felice	- 0.9	- 4.2	- 5.2	- 1.0	- 4.3	0.6	17.8	425	99	0
71	Edith	21.6	- 3.0	- 2.6	+ 0.4	- 24.2	19.9	19.2	376	-9	0
74	Carmen	14.5	7.3	- 1.2	- 8.5	- 15.7	12.9	15.6	385	-43	35
75	Caroline	- 5.8	- 3.0	- 3.9	- 0.9	+ 1.9	6.1	17.9	423	109	30
75	Eloise	6.8	- 3.7	- 5.9	- 2.2	- 12.7	5.0	17.2	378	17	20
77	Anita	4.8	- 2.7	- 3.6	- 0.9	- 8.4	3.8	17.8	417	54	10
77	Babe	4.9	- 1.0	- 3.4	- 2.4	- 8.3	2.1	17.0	418	46	20
	Average	7.1	- 1.0	- 3.8	- 2.8	- 10.8	7.6	17.5	407	51	19

TABLE 9

Summary of the parameters analyzed for the non-intensifying systems at the LF -18 time period

YR	STORM NAME	$\bar{U}_{200}$	$\bar{U}_{500}$	$\bar{U}_{850}$	$\bar{U}_{850} - \bar{U}_{500}$	$\bar{U}_{850} - \bar{U}_{200}$	6° BELT $\bar{U}_{200}$	$\bar{T}_{850}$	$\bar{H}_{200}$	IP	NEXT 24 HOUR WIND SPEED CHANGE
57	Debbie	23.0	10.7	1.5	- 9.2	- 21.5	21.5	16.3	283	-124	0
57	Esther	15.3	2.6	- 0.9	- 3.5	- 16.2	10.4	16.9	377	1	0
58	Ella	10.6	- 4.6	- 8.8	- 4.2	- 19.4	13.3	17.1	453	6	- 5
59	Arlene	16.0	1.1	- 2.9	- 4.0	- 18.9	10.5	16.7	328	28	5
59	Irene	19.6	7.0	1.0	- 6.0	- 18.6	12.8	15.2	338	-23	15
60	TS #1	- 1.7	- 9.0	- 2.2	6.8	- 0.5	- 8.3	18.5	427	185	25
60	Florence	7.2	- 2.9	- 6.5	- 3.6	- 13.7	10.3	13.9	357	-32	- 5
64	TS #1	31.4	9.8	- 1.9	-11.7	- 33.3	30.1	14.6	224	-146	5
65	TS #1	13.8	7.1	5.7	- 1.4	- 8.1	16.8	18.5	293	17	10
68	Gladys	17.3	4.5	- 2.7	- 7.2	- 20.0	13.6	14.3	341	-8	5
69	Jenny	23.7	2.7	- 6.4	- 9.1	- 30.1	24.0	14.1	380	-77	0
70	Alma	19.7	0.1	- 4.9	- 5.0	- 24.6	25.2	14.6	246	-58	0
72	Agnes	16.8	- 1.6	- 9.1	- 7.5	- 25.9	15.2	15.9	379	-23	10
	Average	16.4	2.0	- 2.9	- 5.1	- 19.3	15.0	15.9	340	-37	5

TABLE 10

Summary of the parameters analyzed for the non-intensifying systems at the LF -42 time period

YR	STORM NAME	$\bar{U}_{200}$	$\bar{U}_{500}$	$\bar{U}_{850}$	$\bar{U}_{850} - \bar{U}_{500}$	$\bar{U}_{850} - \bar{U}_{200}$	$\frac{6}{U_{200}} \text{BELT}$	$\bar{T}_{850}$	$\bar{H}_{200}$	IP	NEXT 24 HOUR WIND SPEED CHANGE
57	Debbie	11.2	2.0	- 2.6	- 4.6	- 13.8	8.3	18.3	406	19	0
57	Esther	7.4	2.1	- 2.7	- 4.8	- 10.1	5.0	18.6	404	51	20
58	Ella	8.5	- 5.3	- 9.8	- 4.5	- 18.3	8.1	17.1	422	4	0
59	Arlene	11.0	- 3.0	- 5.8	- 2.8	- 16.8	4.2	15.5	353	52	15
59	Irene	9.7	4.7	- 1.7	- 6.4	- 11.4	8.3	16.6	416	59	10
60	TS #1	- 0.6	- 4.2	- 2.9	+ 1.3	- 2.3	0.3	17.7	406	128	0
60	Florence	12.9	- 1.5	- 5.3	- 3.8	- 18.2	16.5	13.6	323	-88	- 5
64	TS #1	32.4	8.6	- 2.6	- 11.2	- 35.0	29.1	15.5	301	-102	0
65	TS #1	18.2	7.4	3.6	- 3.8	- 14.6	21.0	18.0	331	-2	10
68	Gladys	13.1	1.2	- 7.5	- 8.7	- 20.6	13.0	14.6	344	-8	0
69	Jenny	28.4	6.5	- 1.7	- 8.2	- 30.1	28.0	14.4	356	-93	0
70	Alma	28.7	2.2	- 9.1	- 11.3	- 37.8	26.0	15.0	343	-55	- 5
72	Agnes	15.5	- 3.5	-10.6	- 7.1	- 26.1	15.4	16.5	374	-19	-10
Average		15.1	1.3	- 4.5	- 5.8	- 19.6	14.1	16.3	368	-15	3

TABLE 11

Summary of the parameters analyzed for the independent intensifying systems  
for a period approximately 24 hours prior to landfall

YR	STORM NAME	DATE	$\bar{U}_{200}$	$\bar{U}_{500}$	$\bar{U}_{850}$	$\bar{U}_{850} - \bar{U}_{500}$	$\bar{U}_{850} - \bar{U}_{200}$	$6^{\circ}\text{BELT}$ $\bar{U}_{200}$	$\bar{T}_{850}$	$\bar{H}_{200}$	IP	NEXT 24 HOUR WIND SPEED CHANGE
73	Delia	4 Sep	12.2	-3.7	-5.6	-1.9	-17.8	10.7	17.7	422	11	0
75	DEP #9	28 Jul	10.1	3.6	1.0	-2.6	- 9.1	9.7	17.3	370	15	10
78	Amelia	30 Jul	+ 0.6	-1.7	1.2	2.9	0.6	3.3	18.8	397	86	20
78	Debra	28 Aug	11.4	3.4	-2.4	-5.8	-13.8	13.7	19.6	424	6	25
79	Bob	10 Jul	12.2	3.6	-0.2	-3.8	-12.4	10.3	17.9	400	27	30
79	Frederic	12 Sep	8.3	-5.4	-7.3	-1.9	-15.6	9.7	16.8	433	17	25
79	Henri	16 Sep	11.4	2.2	-6.0	-8.2	-17.4	5.7	15.9	475	39	25
	Average		9.5	0.3	-2.7	-3.0	-12.2	9.0	17.7	417	29	19

TABLE 12

Summary of the parameters analyzed for the independent intensifying systems  
for a period approximately 48 hours prior to landfall

YR	STORM NAME	DATE	$\bar{U}_{200}$	$\bar{U}_{500}$	$\bar{U}_{850}$	$\bar{U}_{850} - \bar{U}_{500}$	$\bar{U}_{850} - \bar{U}_{200}$	$\frac{6^{\circ}\text{BELT}}{\bar{U}_{200}}$	$\bar{T}_{850}$	$\bar{H}_{200}$	IP	NEXT 24 HOUR WIND SPEED CHANGE
73	Delia	3 Sep	10.1	-4.7	-7.6	-2.9	-17.7	9.0	17.3	426	13	20
78	Debra	27 Aug	4.6	1.8	-2.8	-4.6	- 7.4	4.0	18.5	428	38	0
79	Bob	9 Jul	16.4	-0.2	2.0	2.2	-14.4	16.3	17.8	427	40	15
79	Frederic	11 Sep	13.2	-3.8	-4.8	-1.0	-18.0	12.0	16.4	414	-7	25
79	Henri	15 Sep	8.2	3.6	-1.6	-5.2	- 9.8	4.7	16.7	451	63	15
	Average		10.5	-0.7	-3.0	-2.3	-13.5	9.2	17.3	429	29	15

TABLE 13

Summary of the parameters analyzed for the independent non-intensifying systems  
for a period approximately 24 hours prior to landfall

YR	STORM NAME	DATE	$\bar{U}_{200}$	$\bar{U}_{500}$	$\bar{U}_{850}$	$\bar{U}_{850} - \bar{U}_{500}$	$\bar{U}_{850} - \bar{U}_{200}$	$6^{\circ}\text{BELT}$ $\bar{U}_{200}$	$\bar{T}_{850}$	$\bar{H}_{200}$	IP	NEXT 24 HOUR WIND SPEED CHANGE
68	DEP <sup>1</sup>	4 Jul	14.4	4.2	-0.7	-4.9	-15.1	10.3	14.6	342	-39	0
68	DEP	27 Aug	15.6	4.9	1.0	-3.9	-14.6	12.7	16.4	308	-80	0
69	DEP	20 Sep	20.0	5.3	-3.6	-8.9	-23.6	17.7	15.6	346	-76	0
69	DEP	30 Sep	13.6	-1.8	-6.2	-4.4	-19.8	11.3	16.2	292	-60	0
71	DEP	7 Aug	4.9	-0.6	0.6	+1.2	- 4.3	- 0.7	15.8	384	24	0
71	DEP	31 Aug	10.8	1.0	-2.9	-3.9	-13.7	8.0	15.8	390	-30	0
71	DEP	13 Oct	34.0	11.4	2.4	-9.0	-31.6	31.3	14.1	193	-192	0
73	DEP	10 Sep	18.0	4.2	-0.9	-5.1	-18.9	16.7	17.1	452	-5	0
74	DEP #5	17 Jul	-5.1	-4.2	-1.1	+3.1	4.0	- 3.0	17.8	349	77	0
74	DEP #12	25 Aug	9.2	-4.6	-4.1	+0.5	-13.3	8.0	16.6	364	-24	0
74	DEP #20	26 Sep	33.4	14.4	2.9	-11.5	-30.5	32.3	13.9	277	-175	0
75	DEP #9	28 Jul	10.1	3.6	1.0	-2.6	- 9.1	9.7	17.3	370	5	0
75	DEP #22	15 Oct	15.8	5.1	-1.7	-6.8	-17.5	12.0	16.2	296	-31	0
76	DEP #14	6 Sep	10.6	-1.9	-3.7	-1.8	-14.3	9.3	15.7	258	-77	0
76	DEP #17	23 Sep	30.9	13.1	4.2	-8.9	-26.7	29.0	13.5	261	-176	0
77	DEP #2	13 Jun	15.0	3.6	1.1	-2.5	-13.9	12.3	18.7	339	64	0
77	DEP #3	18 Jul	5.9	-5.3	-6.0	-0.7	-11.9	8.0	16.7	410	20	0
77	DEP #19	24 Oct	32.6	10.1	-1.9	-12.0	-34.5	30.3	13.2	142	-209	0
78	DEP #5	21 Jun	10.9	-0.9	-1.4	-0.5	-12.3	8.3	15.7	347	27	0
78	DEP #9	9 Aug	11.9	1.9	-1.3	-3.2	-13.2	9.0	16.3	372	-55	0
78	DEP #18	9 Sep	15.4	2.7	-1.8	-4.5	-17.2	16.3	16.9	414	-20	0
79	Claudette	24 Jul	11.3	3.4	-4.0	-7.4	-15.3	7.7	19.4	493	51	10
79	Elena	31 Aug	10.9	4.0	-2.6	-6.6	-13.5	9.0	18.3	404	-7	0
79	Henri	23 Sep	20.2	7.6	3.0	-4.6	-17.2	14.3	15.4	379	-28	0
	Average		15.4	3.4	-1.2	-4.6	-16.6	13.3	16.1	341	-42	0.4

<sup>1</sup>DEP represents a storm in the depression stage (max wind  $\leq$  34 knots). Prior to 1974, depressions were not numbered.

TABLE 14

Summary of the parameters analyzed for the independent non-intensifying systems  
for a period approximately 48 hours prior to landfall

YR	STORM NAME	DATE	$\bar{U}_{200}$	$\bar{U}_{500}$	$\bar{U}_{850}$	$\bar{U}_{850} - \bar{U}_{500}$	$\bar{U}_{850} - \bar{U}_{200}$	$\frac{6^{\circ}\text{BELT}}{\bar{U}_{200}}$	$\bar{T}_{850}$	$\bar{H}_{200}$	IP	NEXT 24 HOUR WIND SPEED CHANGE
68	DEP <sup>1</sup>	26 Aug	10.7	-0.1	-0.9	- 0.8	-11.6	7.0	17.1	377	-10	0
69	DEP	19 Sep	11.2	-1.3	-7.4	- 6.1	-18.6	8.0	16.6	396	0	0
71	DEP	30 Aug	10.0	-1.1	-2.1	- 1.0	-12.1	5.0	16.5	394	-17	0
71	DEP	12 Oct	27.0	7.4	-1.4	- 8.8	-28.4	24.7	14.1	231	-149	0
73	DEP	9 Sep	15.9	1.1	-4.1	- 5.2	-20.0	9.2	17.6	469	24	0
74	DEP #5	16 Jul	0.6	-1.9	-2.8	- 0.9	- 3.4	2.0	17.7	366	55	0
74	DEP #12	24 Aug	3.9	-4.8	-3.9	+ 0.9	- 7.8	2.7	16.3	384	11	0
74	DEP #20	25 Sep	19.3	15.1	-1.0	-16.1	-20.3	13.0	15.8	392	-49	0
75	DEP #22	14 Oct	11.2	-2.6	-5.9	- 3.3	-17.1	10.3	15.3	337	-6	0
76	DEP #14	5 Sep	13.4	2.1	-0.3	- 2.4	-13.7	11.7	15.8	297	-64	0
76	DEP #17	22 Sep	32.8	12.0	1.7	-10.3	-31.1	33.7	13.3	251	-219	0
78	DEP #19	8 Sep	15.6	4.2	-3.6	- 7.8	-19.2	15.7	16.6	393	-43	0
79	Claudette	23 Jul	10.6	-1.7	-3.6	- 1.9	-14.2	9.3	18.2	446	42	5
79	Elena	30 Aug	15.6	2.4	-1.8	- 4.2	-17.4	9.0	18.1	409	-12	10
79	Henri	22 Sep	19.1	9.1	3.2	- 5.9	-15.9	13.7	15.6	419	-1	0
Average			14.5	2.7	-2.3	- 4.9	-16.7	11.7	16.3	371	-29	<u>1</u>

<sup>1</sup>DEP represents a storm in the depression stage (max wind  $\leq$  34 kts). Prior to 1974 the depressions were not numbered.

## APPENDIX B

## COMPUTATIONAL PROCEDURES FOR THE INTENSITY CHANGE FORECASTING PARAMETER

The computation of the intensity change parameter (IP) has been designed so that it could be performed quickly and with data available at any weather station. It uses the standard isobaric 850, 500, and 200 mb charts which are available twice daily. With only a minimum of practice the IP could be computed in less than 15 minutes using the following guidelines:

1. Locate the storm center on the 850, 500 and 200 mb charts based on the position given by the Miami Hurricane bulletin (or the bulletin issued by JTWC) for a particular time period.
2. Using a compass mark off the 6, 8, and 10° radial belts on the north side of the storm.
3. Subdivide these radial belts into the 45° octants 8, 1 and 2 as in Fig. 2. For storms affecting the eastern U.S., China, Korea or Japan use octants 1, 2 and 3.
4. Compute average values of the parameters  $\bar{T}_{850}$ ,  $\bar{H}_{200}$ ,  $\bar{U}_{850}$ ,  $\bar{U}_{500}$  and  $\bar{U}_{200}$  over the 5-11° belt over octants 8, 1 and 2 (or 1, 2 and 3) by:
  - a. Obtain an average value in each octant for each of the 5-7°, 7-9° and 9-11° radial belts.
  - b. Average the values from each octant in each radial belt to get three belt averages.
  - c. Average these three belt averages together and the resultant number represents the 5-11° belt average over the desired octant.

A quick streamline analysis may have to be done to make it easier to resolve the zonal wind components. When the wind components have been determined in knots, divide by 2 to get the wind speed in  $\text{m s}^{-1}$ . It is helpful to use a table such as those found in Appendix A to keep track of all parameters.

5. Calculate the 850 to 500 mb and 850 to 200 mb wind shears from the table.

6. Using either the graph in Fig. 45 or 46 plot each of the final parameters on the appropriate scale and read off the value from the bottom of the graph. Addition of these five numbers yields the intensity change parameter (IP).

Further refinements can be made in the Atlantic basin based on the seasonal variations described in section 4.2. The adjustments to be made to IP are given in Table 15. After all computations and adjustments have been made, if  $IP > 0$  we should expect an intensifying system. Negative values would represent a filling or steady storm.

TABLE 15

Correction factors to be applied to IP based on seasonal variation. Apply the appropriate correction based on date of occurrence of the cyclone system.

TIME PERIOD	MAY 15-31	JUN 1-15	JUN 16-30	JUL 1-15	JUL 16-31	AUG 1-15	AUG 16-31	SEP 1-15	SEP 16-30	OCT 1-15	OCT 15-31
ADJUSTMENT FACTOR	+80	+50	+20	-10	-30	-50	-50	-30	-10	+20	+50

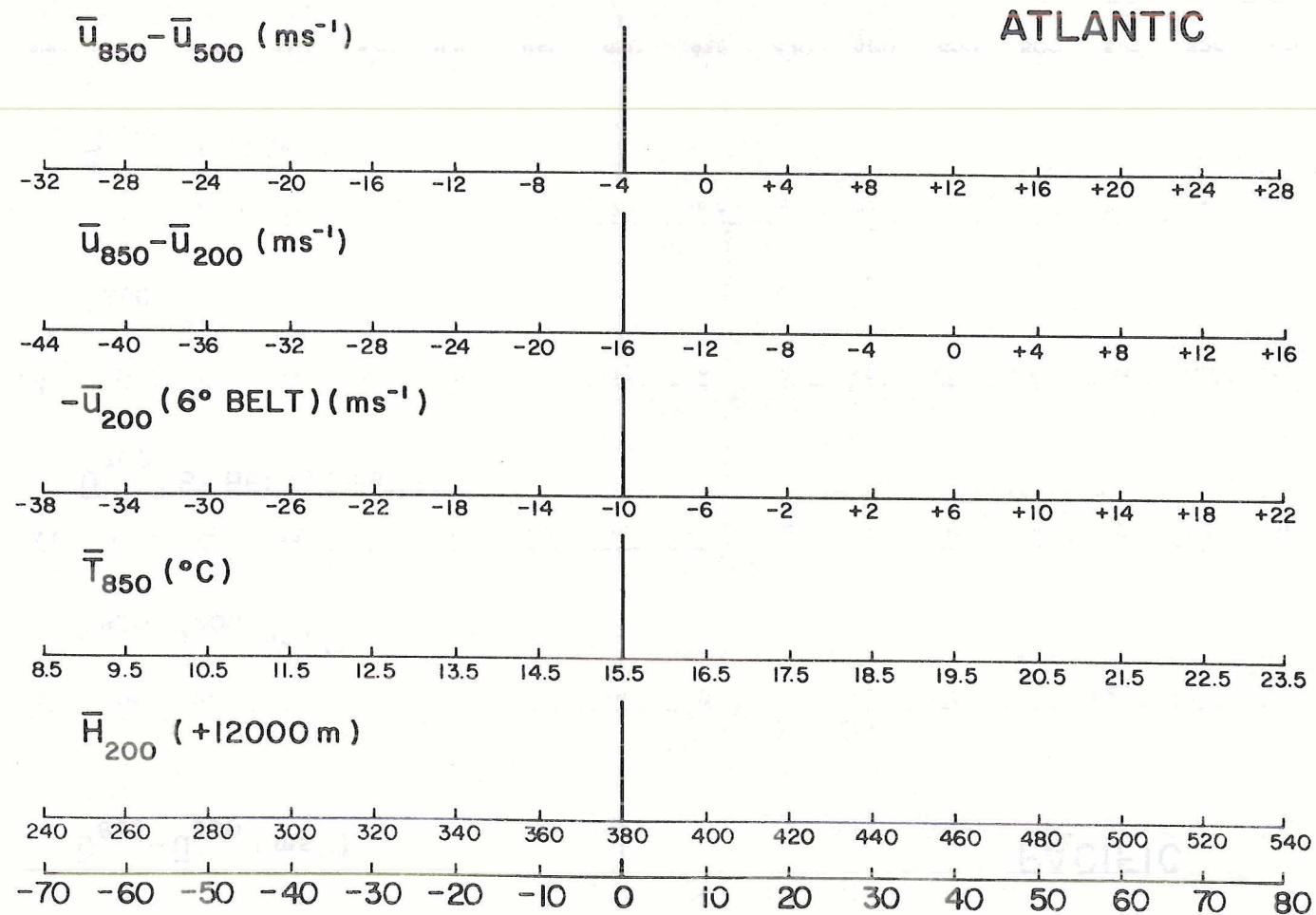


Fig. 45. Computation graph for IP in the Atlantic basin.

# PACIFIC

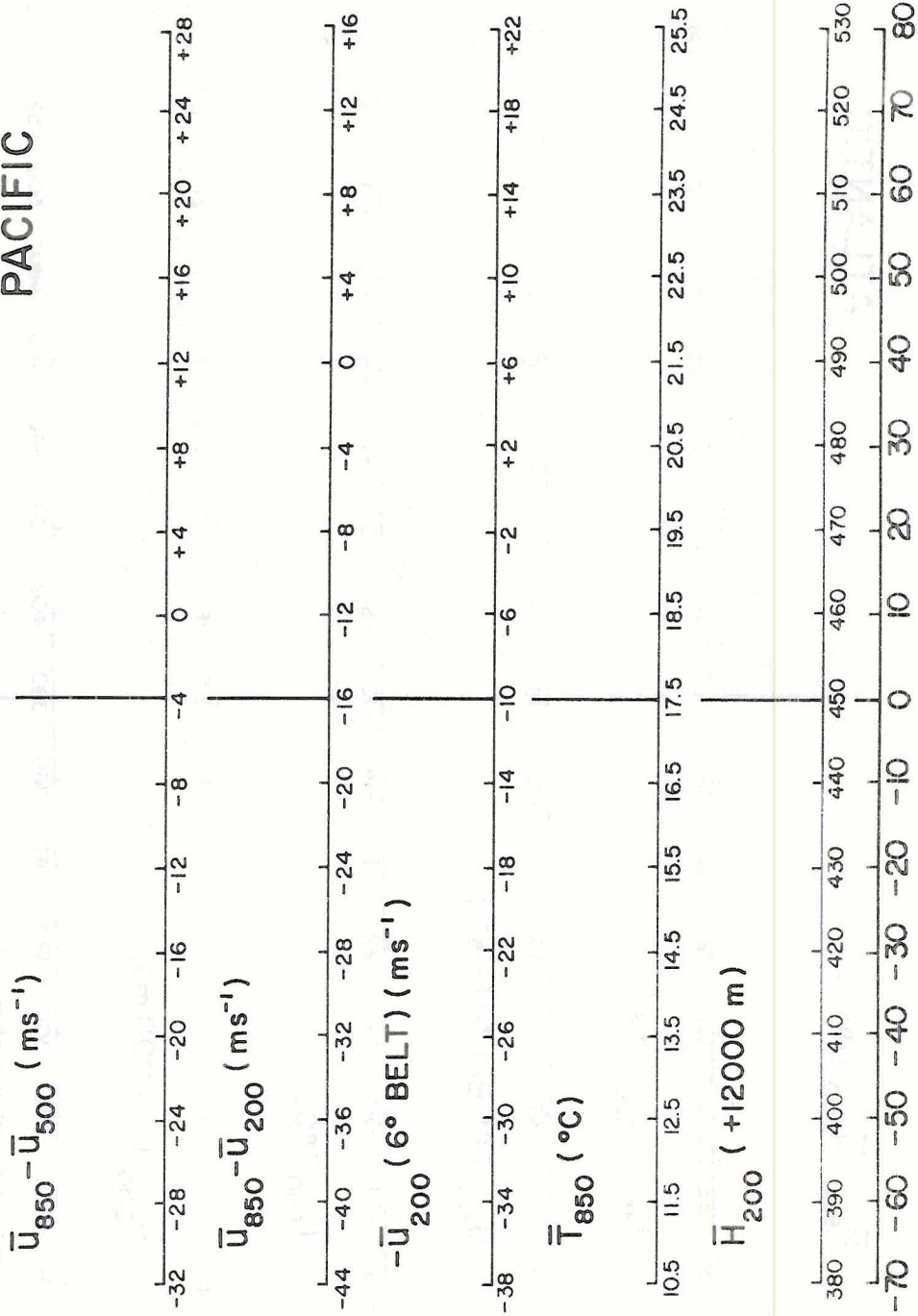


Fig. 46. Computation graph for IP in the Pacific basin.

## APPENDIX C

## DESCRIPTION OF COMPOSITE DATA SETS

Dropco Intensifying: Tropical storms and hurricanes which either formed or moved into the Gulf of Mexico and showed significant intensification (wind speed change  $>20$  kts in 24 hours) prior to landfall along the U.S. gulf coast. The data came from the official best track position of the National Hurricane Center for the years 1957-1977 and include 22 cases. The stratification was based primarily on wind speed change and central pressure when available. The composite was run for two time periods: 42 hours prior to landfall with average latitude =  $23.3^{\circ}\text{N}$ , longitude =  $88.4^{\circ}\text{W}$  and 18 hours prior to landfall with latitude =  $25.1^{\circ}\text{N}$ , longitude =  $90.7^{\circ}\text{W}$ .

Dropco Non-intensifying: Tropical storms and hurricanes which either formed or moved into the Gulf of Mexico and showed little or no tendency for intensification prior to landfall. The data were selected from the best track position of the National Hurricane Center for the years 1957-1977 and include 13 cases. The stratification was made as in the intensifying case and was also run for two time periods: 42 hours prior to landfall with latitude =  $23.8^{\circ}\text{N}$ , longitude =  $84.7^{\circ}\text{W}$  and 18 hours prior to landfall with latitude =  $25.4^{\circ}\text{N}$ , longitude =  $88.0^{\circ}\text{W}$ .

Holliday (1979) rapidly Deepening: Storms from the Northwest Pacific for the years 1961-1970 where 24 hour deepening rate was  $\geq 42$  mb day<sup>-1</sup>. The data were stratified into three periods: 24 hours prior to the onset of rapid deepening, the period at onset, and 24 hours after the onset of deepening.

Bill Frank (1976) Pacific Data Sets: These data sets were made from ten years (1961-1970) of Northwest Pacific rawinsonde data. The data were stratified by both latitude and tendency in the following manner:

Type I  $P_c^1 \leq 980$  mb

Type II  $980 \text{ mb} < P_c \leq 1000$  mb

Type III  $P_c > 1000$  mb

Type A Storm which at some point reaches  $P_c \leq 970$  mb

Type A Early Same as Type A but  $980 \text{ mb} < P_c \leq 1000$  mb and in a deepening trend towards a typhoon.

Type B Storm with  $980 \text{ mb} < P_c \leq 1000$  mb but  $P_c$  never drops below 980 mb.

$l_{P_c}$  represents central pressure of the storm.

Bill Frank (1976) West Indies Data Sets: These data sets were made from 14 years (1961-1974) of western Atlantic rawinsonde data. The data were stratified by latitude and filling or deepening tendencies as taken from the best track positions of the National Hurricane Center.

Zehr (1976) Developing Trade Wind Clusters: Pre-typhoon disturbances found in the trade wind belt taken from the time they were first identified as cloud clusters until they attained an intensity with maximum sustained winds of 50 knots. The data were taken from the central and western North Pacific during the ten year period 1961-1970.

Zehr (1976) Stage 0 Non-developing Cluster: Non-developing cloud clusters in the central and western Pacific for the period 1967-1968. The clusters were found in the region from the equator to  $18^{\circ}\text{N}$  and  $125^{\circ}\text{E}$  to  $160^{\circ}\text{W}$ .

Faint, illegible text at the top of the page, possibly bleed-through from the reverse side.

Vertical text or mark on the right side of the page.

Small mark or characters on the right edge.

Small mark or characters on the right edge.

Small mark or characters on the right edge.